FY 2018 Annual Report and
8th Quarter Research Performance Progress Report

Project Title:	Pore Scale Control of Gas and Fluid Transport at Shale Matrix-Fracture Interfaces
Project Period:	10/01/16 – 09/30/18
Reporting Period:	10/1/17 – 9/30/18
Submission Date:	11/30/2018
Recipient:	SLAC National Accelerator Laboratory
Recipient DUNS #:	00-921-4214
Address:	2575 Sand Hill Road, MS 69 Menlo Park, CA 94025
Website (if available)	www-ssrl.slac.stanford.edu
Award Number:	FWP 100211
Awarding Agency:	DOE/NETL

Principal Investigator: Dr. John Bargar
Senior Staff Scientist
SLAC National Accelerator Laboratory
Phone: 650-926-4949
Email: bargar@slac.stanford.edu

Co-Principal Investigators: Dr. Gordon E. Brown, Jr.
Dr. Kate Maher
Dr. Anthony Kovscek
Dr. Mark Zoback

NETL Project Manager: David Cercone

TABLE OF CONTENTS

1. MOTIVATION, PRIORITY RESEARCH NEEDS, AND ACCOMLISHMENTS

Hydraulic fracture stimulation of unconventional shales to produce natural gas and oil has expanded rapidly in the past decade [1-2] with major benefits to U.S. national energy security. Crucially, however, unconventional fracture stimulation remains highly inefficient, leaving an estimated 95% of oil and 75% of gas resources in reservoirs [3]. This inefficiency exacerbates environmental impacts of unconventional fracture stimulation and places significant demands on freshwater supplies (the dominant stimulation fluid in the U.S.), particularly in the Western U.S. [4-5]. Improving efficiency therefore provides a high-impact path to reducing impacts to the environment and water supplies. Improving efficiency is a high-priority research target.

Precipitation of mineral scale reduces fracture conductivity and matrix permeability [6-7] and is therefore highly significant in the context of efficiency, particularly over the long term. At present, however, we have a poor understanding of geochemical controls over mineral scale in unconventional reservoirs. Knowledge from conventional systems is largely irrelevant in unconventional reservoirs, where strong acids and reactive fluids are injected into and then shut-in for several weeks, creating conditions favorable for fluid-shale reactions and mineral scale formation. We also lack knowledge of the physical-chemical properties of the *altered zone*, which is formed at fracture surfaces wherever injected fluids come into contact and react with shale (**Figure 1**). Loss of permeability in the altered zone has the potential to reduces gas and oil transport throughout the stimulated rock volume.

This R&D project has focused on two sets of interrelated geochemical processes that influence unconventional gas and oil recovery factors: (i) Geochemical controls over mineral scale precipitation in fracture-stimulated shales, which irreversibly clogs porosity and attenuates hydrocarbon production; and (ii) Role and impacts of microstructures in the altered zone (secondary porosity and interfacial or buried mineral scale layers) on shale permeability. These microstructures are formed during reaction with injected fluids and choke recovery factors. Knowledge of such microstructures and their geochemical controls will provide insights and abilities to improve manipulation strategies in ways that will allow industry to intrinsically increase recovery factors. By having a stronger understanding about the important chemical parameters that need to be controlled, new more targeted chemical recipes can and will be developed to aid in mitigating mineral scale production.

Scientific and technical accomplishments during the performance period include:

- Publication of 4 manuscripts, with 3 additional revision or in preparation (Appendix A).
- Presented 5 research papers at national and international meetings, including: URTeC 2018, American Geophysical Union Fall Meeting 2017, and 2017 AIChE annual meeting.
- Filed a provisional patent detailing a new acid formulation to control barite scale
- Forged a research partnership with Pioneer Natural Resources, Inc. to study mineral scale formed during shale-fluid reactions in Midland Basin reservoirs leased by Pioneer. This activity is enriching and advancing our DOE-FE research program by providing detailed knowledge of industrial practices and priorities, credibility with industrial partners, and insights about strategic research priorities.

Five key scientific discoveries have emerged from this work:

1) **Barite scale precipitation can be reduced dramatically with small changes to acid spearhead formulations: Task 2.** In late 2017, we discovered that barite-infused drilling mud (DM) releases large amounts of Ba^{2+} and sulfate (SO_4^{2-}) in the presence of injected hydrochloric acid slugs. This is a highly undesirable process because these solutes dissolved from DM will be pushed out into the formation and precipitate as barite scale that reduces permeability and production. This discovery led to the chemical insight that *we should be able to dramatically reduce barite leaching from DM by making small modifications the acid composition*, specifically by substituting H_2SO_4 for HCl (**Figure 2**). We tested this idea in the laboratory and found that this change reduces barite leaching > 800-fold. Additional experiments and calculations showed that only small amounts of sulfuric acid ($\geq$ 10% H_2SO_4 substitution) are required. Along with addition of citrate ($C_6H_5O_7^{3-}$) to control gypsum formation, barite and gypsum formation were nearly eliminated. Thus, by understanding the fundamental sources of dissolved Ba^{2+} (*i.e.* barite from DM) and the chemical reactions that drive mineral scale precipitation, we can obtain insight that allow proper changes to the injection fluid recipes to be made.

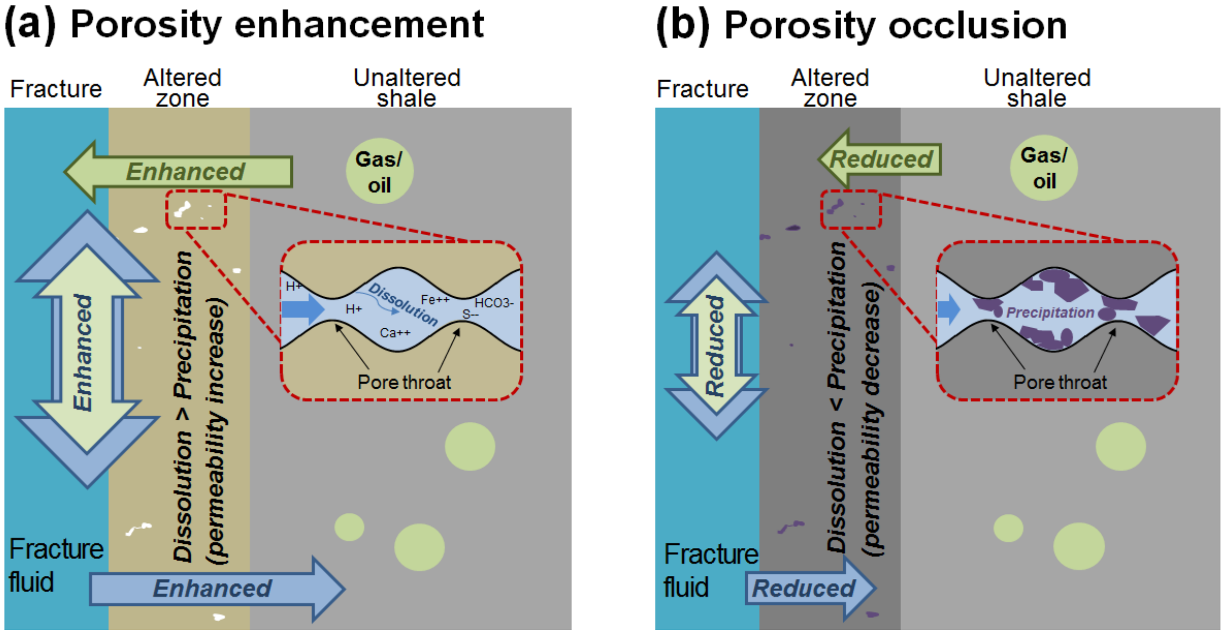

Figure 1: Conceptual model illustrating the altered zone at shale-fluid interfaces and the possible effects of dissolution and precipitation reactions on gas and water flow through the altered fracture surface. Left panel: when shales react with acidic solutions, increased porosity facilitates transport into the shale matrix, resulting in enhanced recovery and favorable extension of pressure gradients into the matrix. Right panel: Precipitation of secondary minerals in the altered zone decreases permeability, leading to less penetration of the pressure gradient in the matrix.

Impact: By optimizing this new barium anti-leaching acid formulation for minimal possible changes to existing industrial practices, this strategy is better poised to gain acceptance by producers and can better support industrial adoption and process improvement.

2) **Validated and enhanced a conceptual model for barium cycling in unconventional reservoirs that can be used to predict and control barite precipitation: Task 2.** Our findings in late FY 2017 that DM releases large amounts of Ba^{2+} and sulfate (SO_4^{2-}) when it reacts with injected hydrochloric acid led us to propose a completely new conceptual model for Ba^{2+} cycling in the stimulated rock volume, driven by barite dissolution and precipitation during injection (**Figure 3**). Our experimental program and thermodynamic calculations, described in highlight 1), have helped to validated this model.

   Impact: validation of this model increases its value for prediction and for optimizing stimulation practices. An excellent example of this predictive value is given in **Task 2**, where a modified barite cycle is predicted to occur when sulfuric acid is substituted for hydrochloric acid to suppress barite leaching. Because radium is incorporated into barite, the barium cycle also has important implications for radium concentrations in flow back water.

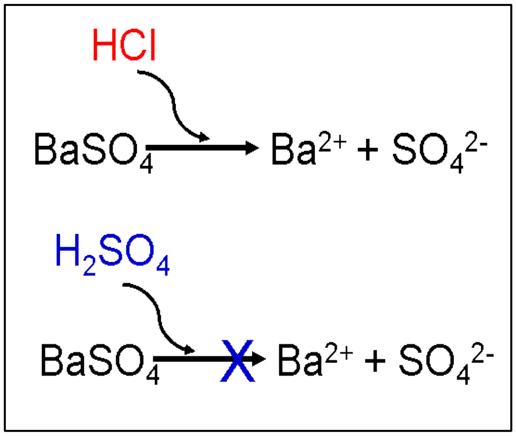

Figure 2. Top row: Barite ($BaSO_4$) dissolution to produce aqueous Ba^{2+} is strongly favorable in the presence of hydrochloric acid (HCl). However, as can been seen in the top row, this chemical reaction requires production of sulfate (SO_4^{2-}). If sulfate is already present in solution at high concentrations, then according to Le Chatelier's Principle, chemical backpressure will inhibit barite dissolution. This idea leads to the insight that barite dissolution can be inhibited by substitution of sulfuric acid for hydrochloric acid (bottom row).

3) **Developed models for geochemical alteration in the altered zone: Tasks 3&4(a) and (c).** Prior to this research, no published studies had quantified the chemical properties of the altered zone (**Figure 1**). Our research has, for the first time, quantified porosity evolution and documented chemical reactions occurring as a function of depth in altered zones occurring in a range of shale types across a range or reaction conditions. Chemical reactions studied include: calcite dissolution, barite scale precipitation, pyrite oxidation, and iron scale precipitation. This work has showed that the altered zone can extend into the matrix by > 0.5 cm within only 3 weeks. Moreover, the thickness of the altered zone and the extent of alteration varies as a function of the type chemical reactions occurring (*e.g.*, dissolution, scale precipitation, sulfide oxidation), the mineralogical composition of the shale, and the shale-fluid interfacial microstructures.

   Impact: This finding indicates that *dissolution within the altered zone provides a means to significantly increase access to matrix, as long as scale precipitation can be controlled*. Thus, one major outcome of this work has been the discovery of chemical behaviors that can be used to manipulate the altered zone to improve permeability and hydrocarbon recovery factors.

4) **Microstructures within the altered zone help control permeability: Tasks 3&4(a) and (b).** Our whole-core experiments show that the presence of microstructures, *i.e.*,

microfractures and very thin coatings of mineral scale, can dramatically alter the extent of chemical reactions and depth of the altered zone. As discussed in Task 3&4(a), the presence of fine microcracks (< 50 µm aperture) dramatically enhance the extent of pyrite oxidation and barite precipitation with shale matrix. Shale cores containing microfractures exhibited relatively deep alteration. On the other hand, the presence of thin (< 40 µm) layers of barite scale on the shale surface significantly reduced development of the alteration zone due to a dramatic diminishment of diffusion across the shale-fluid interface. Gas pulse-decay permeametry measurements (Task 3&4(b)) performed on Marcellus cores exhibiting barite surface coatings showed that permeability was reduced by 20% under reservoir confining and pore pressures as compared to cores that did not contain barite coatings. On the other hand, the permeability of Eagle Ford cores was increased by an order of magnitude due to carbonate dissolution, even when barite scale was present, indicating that the extent and timing of dissolution and scale precipitation are important.

Impact: The finding that specific types of microstructures within the altered zone correlate to specific changes in permeability is very powerful because it provides a basis for targeted chemical manipulation of altered zone properties to improve permeability.

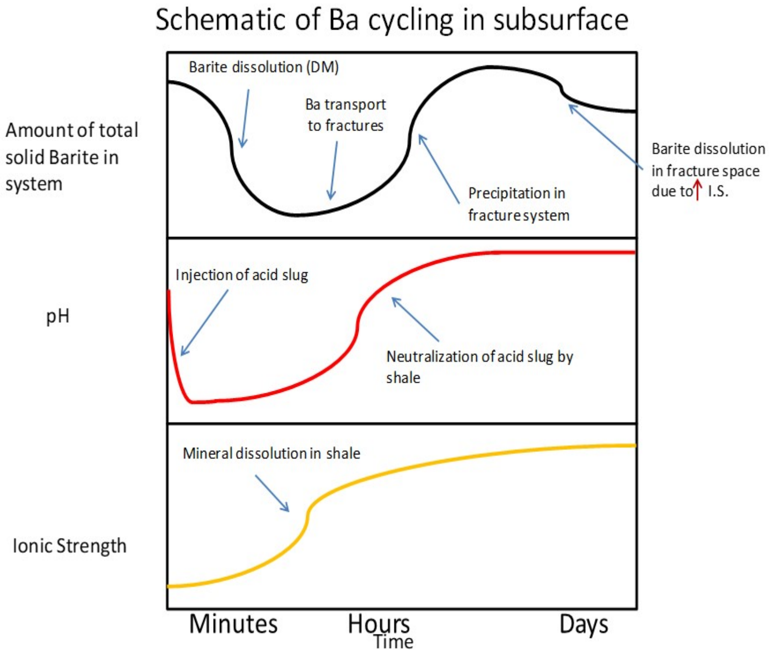

Figure 3. Conceptual model of barium cycling in stimulated shale reservoirs. A 15% hydrochloric acid spearhead is often injected prior to slurry and other fracturing chemicals. This initial acid slug rapidly drives the pH of the system to very low values (pH ~0) (middle panel). As the acid slug interacts with the barite-infused DM, Ba^{2+} and sulfate are released into injected fluids and carried into newly formed fractures in the stimulated rock volume (SRV). Dissolution causes Ba to shift from the solid to dissolved phases, resulting in a significant decrease in the pool of solid-bound Ba (top panel). As carbonates, pyrite, and clays dissolve, the ionic strength of the solution will increase (lower panel). The degree and rate of acid neutralization depends on the amount of carbonate available (carbonate neutralizes acid faster). As acid is neutralized and pH increases, barite will rapidly precipitate on shale surfaces and in matrix. Only a small fraction of this newly precipitated barite scale will be dissolved as I.S. rises to concentrations high enough to promote barite dissolution (upper and lower panels). Though some of the barite will dissolve (releasing trapped Ra), laboratory experiments and thermodynamic models predict < 10% of the precipitated Ba will be released back into solution.

5) **Organics dominated iron reactivity in stimulated reservoirs: Tasks 3&4(c).** Our reaction models indicate that only a very small amount of bitumen is required to dramatically accelerate Fe(II) oxidation by oxygen at low pH during stimulation. The threshold for accelerating oxidation rates is so low that Fe(II) oxidation in virtually all economically important shales will occur at highly accelerated rates controlled by organic-promoted oxidation pathways.

   Impact: Iron scale precipitation results from Fe(II). Consequently, it is not possible to mitigate or otherwise control iron scale without first addressing organic-Fe(II) reactions. On the other hand, the strength of these interactions provides a potential chemical route to accelerating rates of iron oxidation to minimize its spread.

Future directions. Shale reservoirs are fractured using sequential injections of strong acids, sand slurries, and chemical amendments that create strong gradients in pH (0 to 7), salinity (0.1-100 parts per thousand), and dissolved solute concentrations. Injected volumes/rates and concentrations are specific to locations, depths, and commercial operators. Consequently, *chemical conditions in stimulated reservoirs can depart significantly from average model fluids* studied to date. The distinction is important because these factors control thermodynamic stabilities and precipitation rates of mineral scale. Industry wide changes to injection practices in order to improve efficiency can only be accomplished by commercial operators. Consequently, it is important to study and document 'real world' conditions in order for results to have relevance for commercial operators.

Need 1. No studies have investigated unconventional mineral scale formation under 'real-world' chemical condition occurring during chemical injection.

Shale mineralogy/organics and fracture fluid chemistry vary significantly between different shale plays [6, 8]. Several shale regions, such as the Eagle Ford play, contain over 50 wt.% calcite, while other shales, such as Barnett and portions of Marcellus, contain less than 10% carbonate [6, 8-9]. Besides variations in host rock composition and fabric, fracture fluid recipes (both base fluid and chemical additives) vary not only for different regions, but also for different hydrocarbon targets (oil versus natural gas).

Need 2. These variables require a basin-specific investigative approach in which the actual shales found within a local region are matched with base fluids, stimulation practices, and corresponding fracture fluid recipes

To address these needs, this project in FY2019 will begin to investigate scale precipitation that occurs under conditions of actual industry practices. We will also investigate specific chemical strategies to manipulate and enhance production from matrix in different shale types. We will follow a basin-specific approach; Our research program will specifically address and compare reactions occurring in HFTS (Midland basin, Wolfcamp formation) and MSEEL (Marcellus basin, Marcellus formation) reservoirs. Knowledge produced by this work will be encapsulated in conceptual and numerical models, that can be used by industry to improve the efficiency of gas and oil production from unconventional shale reservoirs.

2. GOALS AND OBJECTIVES

This project is conducting fundamental and applied research to address two crucial and interrelated reservoir performance needs that provide the potential to enable industry to deliver significant increases in efficiency:

(i) Reducing scale precipitation through better understanding and control of fundamental geochemical and kinetic factors; and

(ii) Improving microscale knowledge of the fracture-matrix interface required to develop chemical/physical manipulation approaches that can access resource in the matrix.

Over the past year, we have made great progress in achieving these goals through a suite of activities that integrate synchrotron-based imaging and CT methods, electron microscopy, permeability measurements, and geochemical and reactive transport modeling. This approach is providing insights about how to control undesirable mineral scale formation and about the impact of microstructures on shale permeability.

Task 1 encompasses project management activities. The three scientific tasks defined in our project management plan were (**Figure 4**): **Task 2**: Characterizing the influence of dissolved organic compounds, pH, and ionic strength on barite scale precipitation. In contrast, **Tasks 3 and 4** are focused on characterizing and modeling the chemical/microstructural alteration of shale-fracture interfaces and the impact of this alteration on gas transport. **Task 3** was oriented toward porosity generation within the altered layer, whereas **Task 4** was focused on secondary mineral precipitation within the altered layer ('precipitation favorable' conditions). These two chemical processes are interrelated (dissolution leads to precipitation), and the work flows for subtasks 3 and 4 are similar. Consequently, Task 3 and 4 efforts have been merged and are reported as "**Task 3&4**". The merged work flow for **Task 3&4** self-organizes into 3 primary activities: (a) Chemical reactions and sub-core-scale geochemical characterization; (b) permeability measurement, which requires whole-core characterization using core-flood approaches; and (c) numerical modeling of altered shale-matrix interfaces. Results for each are presented separately later in this section. Effort for **Task 3&4** in Year 1 has focused on activities (a) and (b), whereas numerical modeling will be a more significant focus in Year 2.

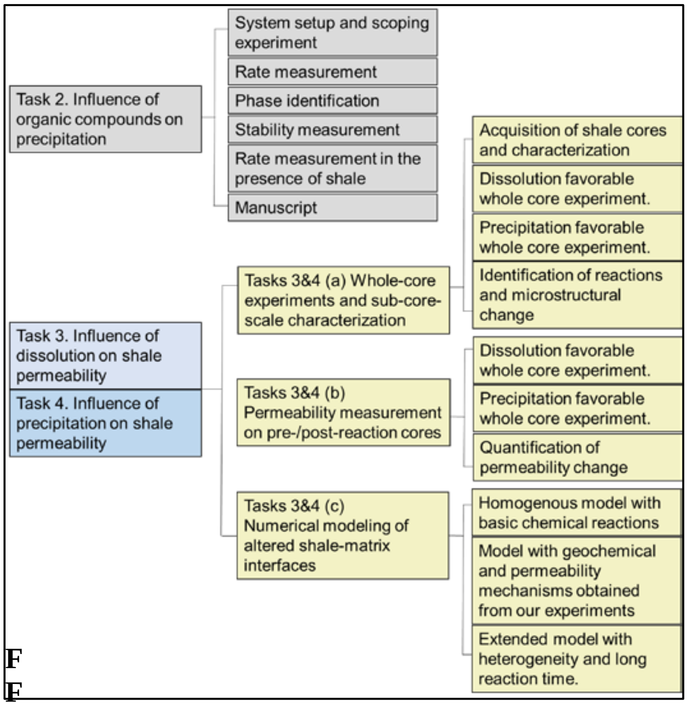

Figure 4. Structure of this report and the relation to PMP tasks. Task 1 (not illustrated) is the program management activity.

3. TECHNICAL HIGHLIGHTS

Task-by-task highlights of accomplishments in Quarter 4 and all of FY 2018:

Task 1

Management in the last quarter of the project focused on recruiting new staff for projects going forward and on wrapping up the science plan for the 2016-2018 project.

Several teleconferences and in-person meetings were held with research scientists at NETL and LBNL to support the ongoing research programs.

Task 2

1. The manuscript associated with this task was submitted to Energy & Fuels for review and potential publication.
2. Patent application
3. Partnership with Pioneer Natural Resources
4. Validation and enhancement of Ba cycling model

Tasks 3 & 4 (a) Fundamental precipitation and dissolution reactions controlling porosity

5. First draft of the planned manuscript is completed.

Tasks 3 & 4 (b) Measuring permeability alteration induced by fracture fluid reaction

6. Micro CT Imaging and segmentation were collected on both post-reaction Marcellus and Eagle Ford samples to identify the depth of the penetration from the reaction fluid front into the altered zone.
7. Porosity calculation from fluid penetration porosimetry measurements on both pre- and post-reaction Marcellus and Eagle Ford samples

Tasks 3 & 4 (c) Numerical simulation of secondary porosity generation and scale precipitation during shale-fluid interactions

8. No highlights in this quarter.

Details of task progress:

Task 1: Project Management

In addition to management activities defined in the PMP, we devoted considerable effort during Quarters 2 and 3 to developing a new basin-specific science plan and preparing a new FWP to conduct this research program. This new FWP outlines 5 major topics:

1. Basin-specific studies of various shale plays reacted with their respective injections chemical suites and injection schedules.
2. Thermodynamic and reactive-transport modeling of results to better develop and simulate new chemical formulations prior to testing in the laboratory.
3. Development of new injection formulas and/or injection strategies to mitigate mineral scale.
4. Development of a new seismic technique to identify development of secondary porosity/mineral precipitation *in-situ*.
5. Tailor chemical suites/injection practices with the goal of increasing hydrocarbon diffusion from the shale matrix through the shale altered zone into fractures.

At the time of writing, we are beginning to undertake this research program.

During FY 2018, we also actively recruited producers with whom we could form a research partnership to help strengthen our knowledge of and connection to industrial practices. In Quarter 7, we engaged in a partnership with Pioneer Natural Resources to investigate the potential geochemical impacts of their stimulation practices on Midland Basin unconventional shales. Wolfcamp shale samples, chemicals, and funding for the Pioneer-related research effort are being provided by Pioneer. Data produced during the study will be disseminated in publications in the open literature after FY 2019. The collaboration with Pioneer has proved to be crucial for developing additional contacts and credibility in the unconventionals industry. The goals of the partnership with Pioneer and its impact on our NETL-funded program are described in greater detail in Task 2 (Progress in Quarters 5-7), which encompasses the scope of this project.

Task 2: Effects of dissolved organic matter on the precipitation and stability of secondary mineral phases

Barite ($BaSO_4$) scale precipitation is a prime concern in nearly all hydraulic fracturing systems, both in shale bodies and in piping. Because of its ubiquitous presence and low solubility, barite tends to be pervasively over-saturated in produced water. Barite is added to drilling muds (DM) at high concentrations (> 10 g/kg) in order to increase the density of the muds and aid in the drilling process [10-12]. Even though some operators attempt to remove as much of the drilling mud as possible, significant amounts of DM is imbedded in the rock during the drilling process remain. This leftover DM can then react with the initial hydrochloric acid slug (~15%) injected down bore hole to clean up perforations in the bore casing and to help clean out the drilling mud. In comparison to the drilling mud, barium concentrations native to the shale host rock are low, typically ≤ 1 g/kg in the solid [12]. The high volume/pressure of the injection fluid and the low pH (~ pH 0), result in a high probability of dissolving and mobilizing Ba from the DM and forcing it into the newly formed fractures as well as the shale matrix itself. This introduction of significant quantities of Ba^{2+} and SO_4^{2-}, including that which is leached from the shale itself, will lead to scale production, clogging of newly developed secondary porosity, and overall attenuation of permeability.

The scope of this task included investigating the effects of various classes of added and natural organics found in hydraulic fracturing systems, including fracture fluid additives (biocides, breakers, crosslinkers, friction reducers, scale inhibitor, Fe-control, corrosion inhibitor, and gellants), as well as those present in shale (both formation and produced waters). The major question being addressed by this task was; How do variations in pH, ionic strength, dissolved organic compounds, and mineral surface area impact Ba release into hydraulic fracturing systems and subsequent barite scale precipitation?

Besides investigating the impact of organics, pH, and I.S. on the precipitation of barite scale, an examination of potentially unknown/ignored sources for Ba^{2+} and SO_4^{2-} to injected stimulation fluids was conducted. The primary driver for this research was the fact that Ba concentrations in the shale (up to 2,000 ppm Ba [13]) are not sufficiently high to account for the extremely high and surprisingly consistent total Ba concentrations found in produced waters [14-16]. Barite in drilling mud has often been considered inert, but our research at the end of FY 2017 [17] showed that the initial acid spearhead/slug (15% hydrochloric acid) at pH ~ -0.3 can dissolve upwards 18% of the barite in drilling mud (20-60 wt.% barite) within hours of interaction. Acid “spearhead” injections are widely used in industry, to the point that it is quite rare to find operators that do not use it. Moreover, through direct discussions with operators on the topic of leftover drilling mud, we have been told that during the drilling process ~1/3 of the drilling mud used is lost to the formation which depending on the borehole can be upwards of 500 barrels of barite-laden drilling mud. **Thus, our research showed that leftover drilling mud has the potential to be a significant, if not the dominant, source of Ba^{2+} and SO_4^{2-} in stimulated unconventional reservoirs through the dissolution of barite added to drilling mud as a weighing agent**.

Table 1: Task 2 objectives for Quarter 8

Goal	Status
Filing of Provisional Patent	Completed

Progress in Quarters 5-7:

Leaching studies of barite-infused drilling mud. Experiments for this study were concluded in late FY 2017. During the first 3 quarters of FY 2018, we wrote and published a peer-reviewed URTeC conference proceedings paper and presented the findings at the 2018 URTeC conference (Houston, TX). These findings also stimulated us to formulate a new conceptual model do describe barium cycling in the SRV, described in section 1 and **Figure 3**.

New approach to mitigating barite scale precipitation in unconventional reservoirs. The discussion on the preceding page emphasizes that a new strategy to mitigate barite scale in unconventional reservoirs is badly needed. One common barite scale control practice in conventional systems (and also in unconventionals) is to add organic compounds to chelate Ba^{2+} and thus retard or interrupt barite precipitation. However, our research in FY 2017 also showed that commonly added organics actually will not chelate Ba^{2+} under slightly supersaturated conditions; In many cases we observed that organics actually accelerate precipitation.

We initiated a series of experiments in FY 2018 to test if barite in the drilling mud could be stabilized by changing the acid composition. If such an approach were to be successful, then it could provide a path to developing a new and industrially compatible/implementable geochemical strategy for reducing Ba precipitation in unconventional reservoirs. Since barite is one of the most important scale minerals, this would be a very important advancement of fracture stimulation practices.

Our new strategy involves stabilizing barite in the drilling mud – before it is dissolved – so that Ba^{2+} and SO_4^{2-} are not released into solution and transported into the newly formed fractures and shale matrix, where they can reprecipitate as barite as the injected acid is neutralized through mineral dissolution, raising the solution pH. As illustrated in section 1 and **Figure 2**, this strategy involves the altering of the acid spearhead/slug from being hydrochloric acid to sulfuric acid of equivalent acidity. The theory is that the excess sulfate will stabilize barite ($BaSO_4$) via the common ion effect and LeChatlier's principle. One drawback to this strategy is that excess sulfate has the potential to cause gypsum precipitation in carbonate-rich shales due to the release of significant quantities of Ca through calcite dissolution. To address this issue, Na-citrate was added to the new acid formulation. Thermodynamic modeling of acid mixtures (hydrochloric and sulfuric) was performed to determine the minimal amount of sulfuric acid that could be used in order to achieve the desired impact. The new chemical formulation was developed to: 1) stabilize barite in drilling mud while keeping overall acidity the same; 2) use relatively inexpensive chemicals so that the capital outlay for operators would be minimal; and 3) use chemicals that operators are already familiar with and are more willing to adopt for use.

Experiments for this project were designed and initiated during quarters 5-7. The results of these experiments are discussed below in the subsequent section,

Progress in Quarter 8.

Provisional patent filing. Following the success of this work, we filed a provisional patent with the United States Patent Office through Stanford University's Office of Technological Licensing to declare our legal ownership of this technology and to help promote its use in industry. The provision patent is entitled, Fracture Fluid Alteration to Mitigate Barite Scale Precipitation in Unconventional Oil/Gas Shale Systems. Patent ID: 62/717326.

We will submit these results for consideration as a presentation and extended abstract/conference paper at the 2019 URTeC conference in Denver, CO.

Collaboration with Pioneer Natural Resources to characterize fluid-shale alteration. During FY 2018, we engaged in a partnership with Pioneer Natural Resources to investigate the potential geochemical impacts of their stimulation practices on Midland Basic unconventional shales. This collaboration has provided invaluable insights into injection chemistry, injection sequences, volumes, and rates that are critical in order to understand what operators are doing in highly complex unconventional oil systems. The collaboration with Pioneer is designed specifically to investigate their specific suite of chemicals on the shale samples they are stimulating using both recycled municipal effluent water and produced water as the base fluids for injection fluids.

Besides using the *exact* chemicals used in the field by industry, the general knowledge of their injection sequence provides insights into geochemical conditions created by injected fluids, which is not possible to gather from the FracFocus database [18]. Our collaboration with Pioneer supports DOE-FE objectives of rapid dissemination of new knowledge and ideas for mitigation strategies to operators in the Midland/Permian/Delaware basins. The partnership also supports the DOE research program by helping us to understand those geochemical challenges that are likely to be roadblocks for industry across the region and U.S. Wolfcamp shale samples, chemicals, and funding for the Pioneer-related research effort is being provided by Pioneer Natural Resources. Data produced during the study will be disseminated in publications in the open literature after FY 2019.

The collaboration with Pioneer has proved to be very helpful for developing additional contacts and credibility in the unconventionals industry. Our work has also garnered interest at Exxon-Mobil, with whom we have had several meetings to discuss and develop an industrial collaboration.

Approach and Results:

New approach to mitigating barite scale precipitation in unconventional reservoirs. A series of 4 reaction sets were completed to compare the effect of using sulfuric acid instead of hydrochloric acid for an acid slug along with whether the addition of citrate could reduce the formation of gypsum in carbonate-rich shales. The concentration of HCl and H_2SO_4 were selected to match the pH of the injected acid slug while citrate concentrations were selected at levels that thermodynamic modeling indicated would be sufficient to halt gypsum formation in a Marcellus system similar to our previous work on Marcellus shale. Drilling mud used for the MSEEL site (Morgantown, WV) was reacted under one of 4 conditions (**Table 2**): 1) 15% hydrochloric acid; 2) 6.3% sulfuric acid; 3) 15% hydrochloric acid + 0.05 M Na-citrate; and 4) 6.3% sulfuric acid + 0.05 M Na-citrate. The reactions were conducted at 80^oC for three days. Solutions were filtered through 20 nm pore size filters and then analyzed for total Ba using ICP-OES.

The total Ba concentration in solution obtained using only sulfuric acid (condition 2) was 170 mg/L, which was orders of magnitude lower obtained using only hydrochloric acid (Condition 1), 149,000 mg/L Ba^{2+}. Thus, switching HCl to H2SO_4 produced an 873-fold drop in barium leaching from drilling mud (**Table 2**). When the reactors containing HCl + Na-citrate (Condition 3) and H_2SO_4 + Na-citrate (Condition 4) are compared, the total drop in released Ba was again 817-fold (**Table 2**). Because citrate is a strong chelator for a variety of metals, it is important to compare the acids with and without citrate to determine if the addition of Na-citrate dissolves additional barite compared to the acid only system. When comparing the ratio of Ba released from drilling mud for HCl vs. HCl + Na-citrate and H_2SO_4 vs. H_2SO_4 + citrate, the ratios are very close to 1, indicating that the citrate has no detectable impact on barite (**Table 2**).

Table 2: Barium leaching reduction factors obtained under various treatments.

pH of all reactors was -0.3.

Acid Comparison	**Ba released A / Ba released B**
HCl / H_2SO_4	873.7
HCl citrate / H_2SO_4 citrate	817.2
HCl no citrate / HCl citrate	1.08
H_2SO_4 no citrate / H_2SO_4 citrate	1.01

To determine whether the addition of citrate was able to control precipitation of gypsum, the experiments on the drilling mud were conducted a second time in which the supernatant was reacted with ground shale. After a subset of solution was taken for ICP-OES analysis, the filtered solution was reacted with 1 g of ground Green River or Marcellus shale (150-250 μm). Due to the extreme acidity of the solution and the low quantity of shale, after full reaction with acid the pH of the solutions was ~0. Since most systems attain a pH of 7, the solutions were titrated to pH = 7 using NaOH in order to allow the precipitation of gypsum due to the release of Ca from the shale. X-ray diffraction patterns measured from the reacted samples were completed to determine the effect of added citrate and excess SO_4 on gypsum precipitation. For samples reacted with the Ba-laden HCl solutions, barite dominated the diffractogram (data not shown) suggesting that Ba and SO_4 liberated from the drilling mud will be transported into fractures and the shale matrix where it will precipitate once pH rises. Conversely, for the Marcellus system (8.5 wt.% calcite) gypsum was not detected in either sulfuric acid containing reactor (sulfuric acid only and sulfuric acid + Na-citrate). This indicates that for carbonate-poor systems (most portions of Marcellus, Barnett) that gypsum precipitation with or without the addition of citrate is of little concern. For high carbonate systems however, gypsum formation is potentially a significant problem. For the Green River shale (55 wt.% carbonate, calcite/dolomite) a significant amount of gypsum precipitated when only sulfuric acid was used (**Figure 5**). However, the addition of 0.05 M Na-citrate resulted in a 90% reduction in gypsum precipitated (**Figure 5**).

Based on experimental results thermodynamic modeling was performed using Visual Minteq [19] to determine the effect of mixing HCl and H_2SO_4 in order to reduce the amount of SO_4 introduced to carbonate-rich systems to further reduce the potential for precipitating gypsum. In all cases (**Figure 6**) HCl is balanced with H_2SO_4 in order to maintain the pH -0.3 preferred by operators. A dramatic drop in Ba released from barite is seen going from 100% to 90% HCl (left side, **Figure 6**). Modeling has also shown that Na-citrate can be as high as 1.5 M before any citrate-bearing phases begin precipitating. Though it would be ideal to always inject with 6.3% sulfuric acid (no hydrochloric acid), even with 1 M Na-citrate some gypsum will precipitate. Calculations indicate that by mixing the two acids at a ratio of 1:1 (effective concentrations of 7.5% HCl and 3.15% H_2SO_4) with 1 M Na-citrate, no gypsum will precipitate regardless of carbonate concentration. This modeling exercise allows us to quickly adjust the acid/citrate mixture depending on the overall shale mineralogy allowing for not only a basin-specific acid spearhead/slug adjustment, but a formation specific formulation. An additional benefit of this formulation is that the additional cost to an operator is minimal since the cost of sulfuric acid is on par with hydrochloric acid and citrate, either Na-citrate or citric acid is fairly inexpensive.

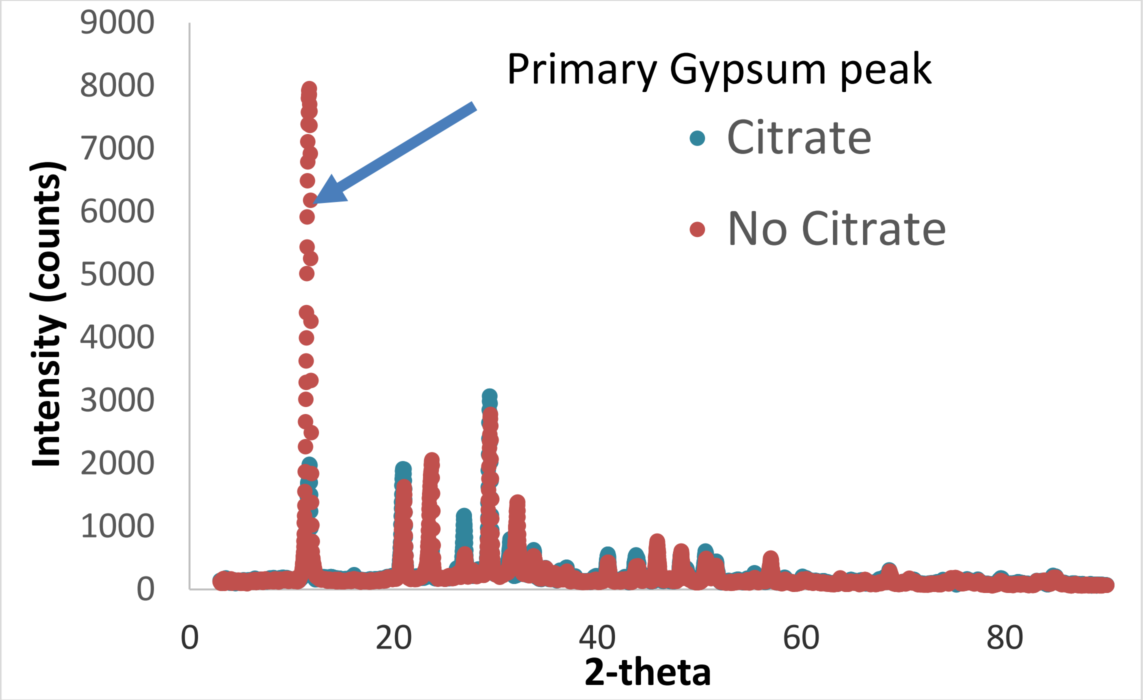

Figure 5: X-ray diffraction data of Green River shale reacted with supernatant from drilling mud reacted with either H_2SO_4 or H_2SO_4 + 0.05 M Na-citrate. The addition of Na-citrate resulted in a 90% reduction in precipitated gypsum, no barite was detected.

New insights regarding actual industry practices (chemical formulations, mixing ratios, injection volumes, injection sequences, injections rates, etc.) are being obtained through our collaboration with Pioneer Natural Resources. Experimental work with this industrial partner is necessary to conduct a true large-scale basin-specific study in which shales from specific basins/plays are reacted with their specific fracturing fluid formulations and injection sequences.

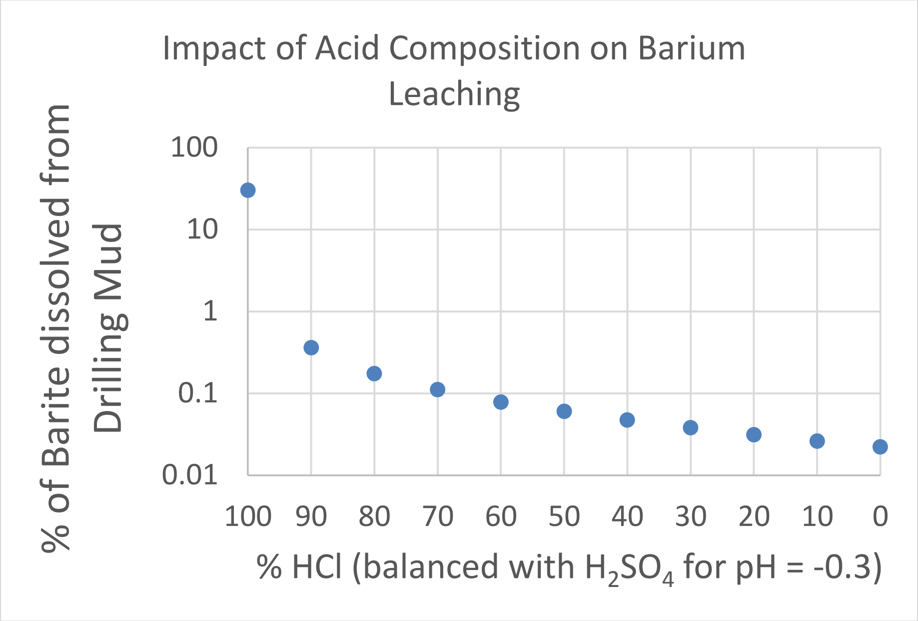

Figure 6: Thermodynamic modeling of barite dissolution in the presence of HCl/H_2SO_4. All calculations were done at $80^{o}C$.

Impact: A new acid formulation that halts barite dissolution from leftover drilling mud while also mitigating gypsum formation was developed and patented. This new technology can be immediately adopted by industry to reduce barite scale precipitation in stimulated unconventional reservoirs. Experimental results have confirmed thermodynamic modeling and has resulted in a refinement of our original Ba cycling model (**Figure 3**) when the new formulation is used (**Figure 7**). Further thermodynamic modeling has resulted in a highly tunable acid formulation that can be adjusted rapidly to compensate for the amount of carbonate in the system.

Results: All planned experimental work defined in the PMP for this task is complete.

Planned Experiments: Starting in FY 2019, we will initiate a new set of experiments to conduct the Basin Specific research project described in Section 1, “Future Directions”. This new study will provide 3 types of findings important to industry as a whole:

1. Identifying the major alterations happening to rocks for a given basin, and different shale units within a given basin, that will be either a benefit (secondary porosity generation) or detriment (mineral scaling) throughout the basin.
2. Identify potential master variables (pH, ionic strength, carbonate content, pyrite, etc.) that can affect secondary porosity and mineral scaling regardless of the basin or stimulation practice.
3. Determining which chemical additives are ineffective, or worse detrimental, to rock permeability and use information for new formulations/mitigation strategies.

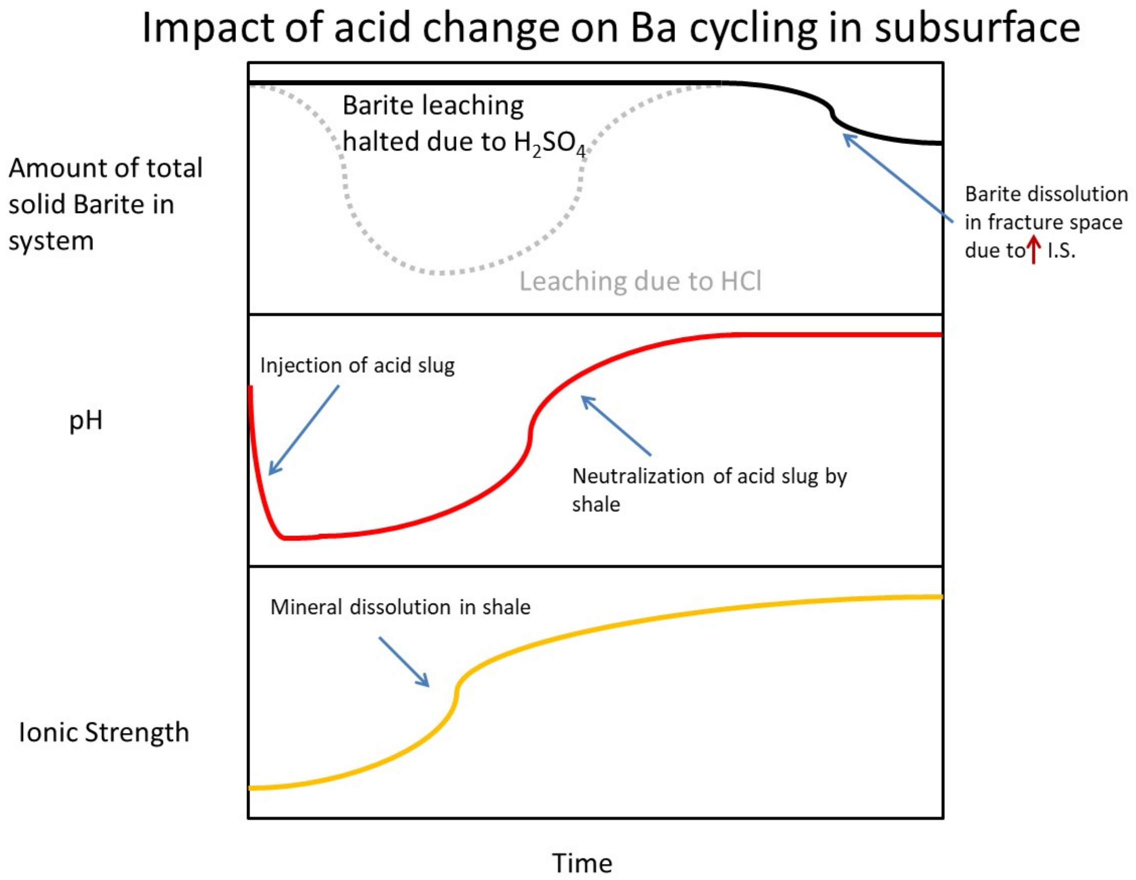

Figure 7: Schematic of theoretical impact on Ba cycle (leaching and precipitation) in the subsurface by substituting 5.6% H_2SO_4 for 15% HCl acid slug/spearhead. Dashed line indicates original curve due to the use of HCl instead of H_2SO_4.

Manuscripts: Experiments performed in FY 2017 to investigate Ba precipitation in the presence of varying pH, I.S., and organics inherent to unconventional shale systems were scheduled to be written and submitted for publication in FY 2018. A manuscript was written on the topic, submitted for review, and is currently being revised to take into account comments from peer-review.

Task 3&4 (a): Fundamental precipitation and dissolution reactions controlling porosity

Shale matrices are the importance media through which hydrocarbons are transported to fractures to be collected. Therefore, any alteration in porosity, permeability, wettability, and pore structure of the shale matrix caused by hydraulic simulation can affect the efficiency of hydrocarbon recovery. Upon exposure to acidic fracture fluid, shale matrices experience mineral dissolution, which leads to an increase in dissolved mineral forming solutes in solution and a slow rise in pH. These changes in solution chemistry ultimately create conditions favorable for secondary mineral precipitation. Thus, these two processes (dissolution and precipitation) compete to alter porosity, diffusivity, and permeability of the matrices, resulting in either an enhancement or reduction in gas/oil production.

The goal of this section (**Task 3&4(a)**) is to *determine alteration zone thickness*, so we understand the length scale in which gas/oil transport is affected by shale-fluid interaction. We reacted whole cores with fracture fluid and characterized them with μ-x-ray CT and synchrotron μ-XRF chemical mapping.

The characterization focuses on four key reactions:

- Carbonate dissolution
- S oxidation following pyrite dissolution
- Fe(II) oxidation following pyrite dissolution
- Barite precipitation

A related task (**Task 3&4 (b)**), focuses on reaction-induced permeability alterations of the shale matrix using laboratory-based porosity and permeability measurements and connected back to this task to relate microstructural changes to permeability. In **Task 3 & 4 (c)**, secondary porosity generation and mineral precipitation is numerically simulated in order to understand the mechanisms of shale-fluid interactions and predict future shale alteration based on initial shale mineralogy.

Progress in Quarters 5-7:

In Quarters 1-4 (FY 2017), we characterized the altered zones for barite precipitation and sulfur oxidation in the Marcellus and Eagle Ford cores. While these tests provided compelling results, it was unclear if they could be viewed as representative of these shale interfaces. Therefore, it was necessary to further confirm the findings in Quarters 5-7. Duplicate experiments were conducted and the samples were characterized for barite precipitation and sulfur oxidation. Combining the main and the duplicate experiments, we now conclude our key findings, focusing on 4 key geochemical processes (**Figure 8**):

- **Barite precipitation:** occurred on the surface of the Pennsylvania Marcellus cores, and within the matrix and microcracks of the Eagle Ford shale. This difference is due to the higher pH in the Eagle Ford system due to dissolution of its higher content of carbonate compared to the Marcellus system.

- **Sulfide oxidation:** occurred throughout the entire thickness of the Pennsylvania Marcellus cores, suggesting that dissolved O_2 migrated efficiently into the entirety of the cores. In contrast, sulfide (dominated by pyrite) oxidation in the Eagle Ford samples was not observed, likely due to O_2 consumption by the competing oxidation of Fe(II), which is much faster in the higher pH environment of the Eagle Ford systems.

- **Iron oxidation:** occurred within a 200 – 300 μm depth zone from the shale-fluid interface into the shale matrix. Eagle Ford has a more distinct Fe(III) oxidation zone than Marcellus because Fe(II) oxidation is faster with higher pH.

- **Carbonate dissolution:** penetrated 150 – 200 μm into the Marcellus matrix, and only ~ 30 μm into the Eagle Ford matrix. This contrasting behavior can be attributed to the low carbonate content in the Marcellus and high carbonate content in Eagle Ford samples.

These processes and findings are summarized graphically in **Figure 8**.

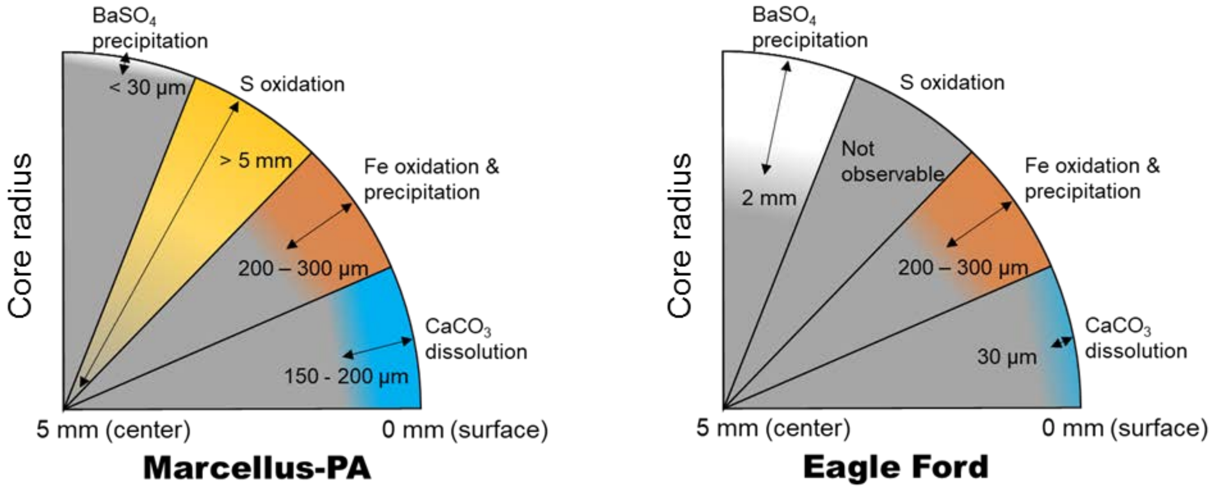

Figure 8. Schematic illustration of cross-sectional wedges of Marcellus and Eagle Ford cores, on which key findings about alteration zone thickness for each of the above noted 4 processes are projected. As illustrated on the core wedge cross-sections, the alteration depths vary depending on the type of process and shale, from 0 mm to 5 mm (complete penetration to core center).

Barite precipitation: The results from duplicate experiments conducted in FY 2018 show great consistency with the first batches of experiments performed in FY 2017. First, barite precipitation occurred in microcracks and the matrix of the Eagle Ford core, and on the surface of the Pennsylvania Marcellus core. The difference of barite precipitation in Eagle Ford and Pennsylvania Marcellus samples are due to their different contents of calcite. Eagle Ford samples have about 50% calcite which quickly dissolved to completely neutralize the initial acidic pH. Findings from **Task 2** manifest that neutral pH promotes more barite precipitation compared to acidic pH. In our Eagle Ford cores, the solid-to-liquid ratios in the pore spaces are higher than that in the solution, rendering faster pH neutralization in these spaces (due to calcite dissolution) and substantial barite precipitation. Therefore, barite precipitation occurred inside the Eagle Ford shale matrix`. In contrast, Marcellus samples have only 1% calcite, and calcite dissolution is not able to neutralize the acid and raise pH enough to accelerate barite precipitation rate. In the Marcellus system, barite precipitated outside of the core matrix with the initial mild oversaturation, before pore space pH could be neutralized by calcite dissolution to enhance barite precipitation. As a result, barite occurred on the surface of the Pennsylvania Marcellus shale core, with some of the precipitates covering the surface of the cores. These contrasting observations in the Eagle Ford and Pennsylvania Marcellus samples highlights the importance of pH and carbonate content for controlling barite precipitation in unconventional reservoirs. Even if the fluid is only mildly oversaturated with barite, substantial barite precipitation may occur inside the matrix, clogging microcracks that are crucial for hydrocarbon migration to the fractures.

Sulfide oxidation: The second key finding confirmed by duplicate experiments is that sulfide oxidation occurred throughout the matrices of the Pennsylvania Marcellus cores, but was not observable in the Eagle Ford cores. The fact that dissolved oxygen could migrate throughout the very low permeability Pennsylvania Marcellus cores indicates that the fracture fluid was imbibed to the very center of the 1 cm core within the three-week time frame of the experiments. Pyrite can be oxidatively dissolved in the presence of dissolved oxygen, producing sulfate anions that may precipitate as sulfate minerals that clog pore spaces, or be adsorbed and modify wettability of the pore walls. In the Eagle Ford, sulfide oxidation was not obvious, likely due to the low content of pyrite (3%) compared to the Marcellus samples (7%). Also, in Eagle Ford, the fluid pH was rapidly buffered to near-neutral pH due to calcite dissolution, resulting in much faster Fe(II) oxidation and Fe(III) (hydr)oxide precipitation that compete with sulfide oxidation for dissolved oxygen. This finding highlights the reactivity of pyrite as a dissolving primary mineral, and its potential to alter pore structure and shale wettability.

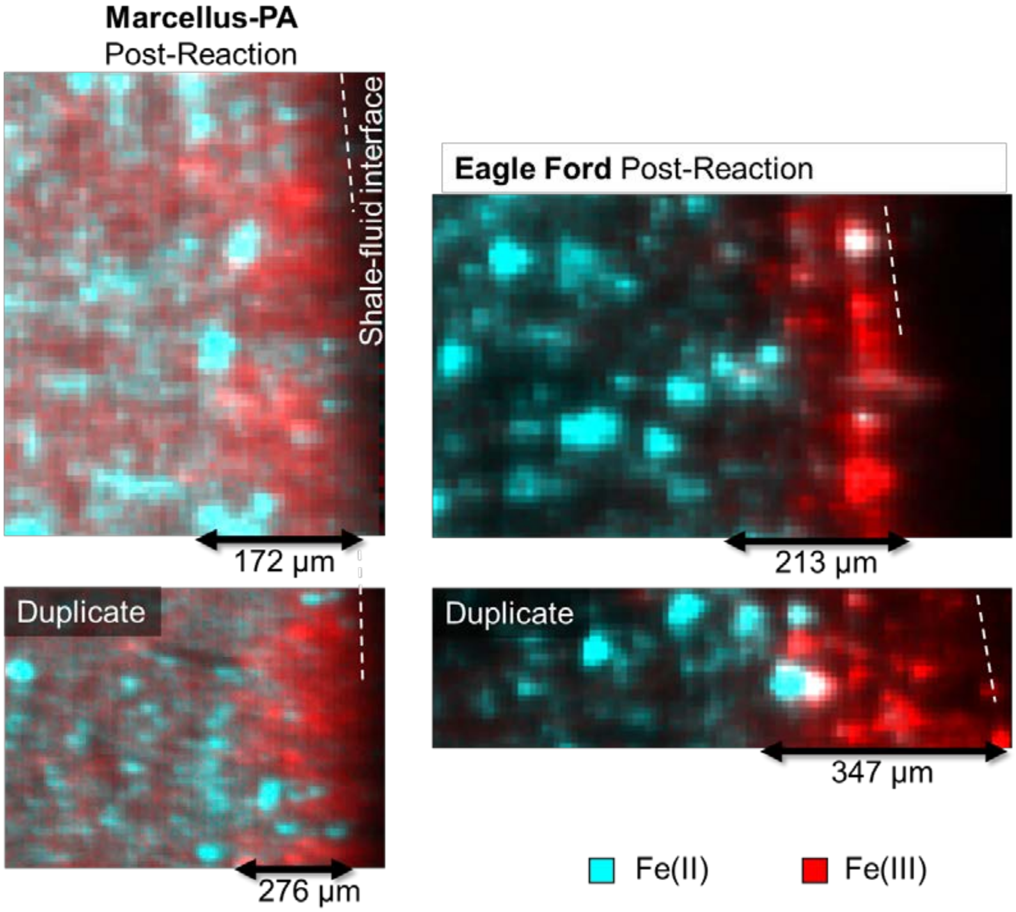

Figure 9. Fe(II) and Fe(III) spatial distribution maps on Pennsylvania Marcellus and Eagle Ford cross sections after reaction with fracture fluid. The white dotted lines indicate where the shale-fluid interface locates. In all circumstances, Fe oxidation occurred 200 – 300 μm into the matrix, forming a Fe(III)-enhanced rim close to the shale-fluid interface.

Iron oxidation: In addition to sulfide oxidation and barite precipitation, we further quantified iron oxidation and calcite dissolution depths in the reacted cores from the original experiment and duplicate experiments. From synchrotron μ-XRF multi-energy maps for Fe, we obtained the spatial distribution of Fe(III) as shown in **Figure 9**. The rim of the cross sections show a higher signal from Fe(III) compared to the middle of the section. The Fe(III)-rich rim was about 200 –

300 μm thick for both Pennsylvania Marcellus and Eagle Ford, in both the original and duplicate experiments. The Fe(III) (oxyhydr-)oxides that precipitates in this rim can potentially occupy the spaces at pore throats, reducing transport of hydrocarbon into the fracture.

Calcite dissolution: Besides Fe oxidation, synchrotron μ-XRF mapping was used to quantify the size of the $CaCO_3$ dissolution regions for Pennsylvania Marcellus. The top image in **Figure 10** shows that Ca was leached in a ~100 μm thick region at the shale-fluid interface, with local width varying according to the initial local calcite content. To observe the secondary

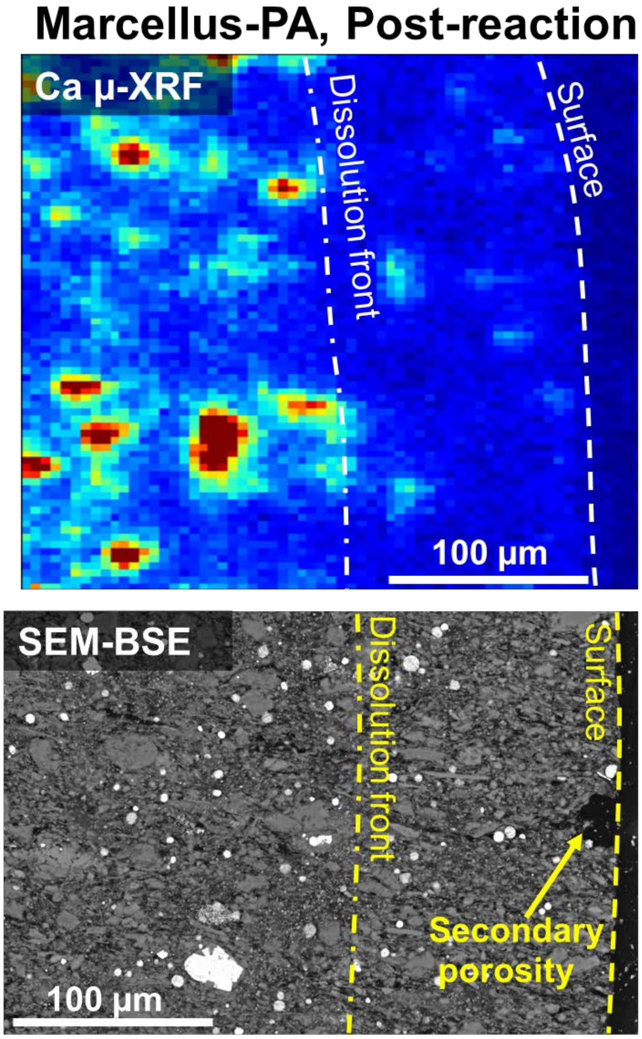

Figure 10. *Top:* Synchrotron μ-XRF maps for Ca from post-reaction Marcellus cross sections. The dotted lines mark the boundaries of the Ca leached zone. *Bottom*: BSE images of post-reaction Marcellus cross sections. Although the cores have ~100 μm deep carbonate dissolution zones (indicated with dotted lines in the BSE image) observed from μ-XRF mapping, the secondary porosity resolvable in the BSE image are localized to calcite grains at the shale surface that have been dissolved during reaction.

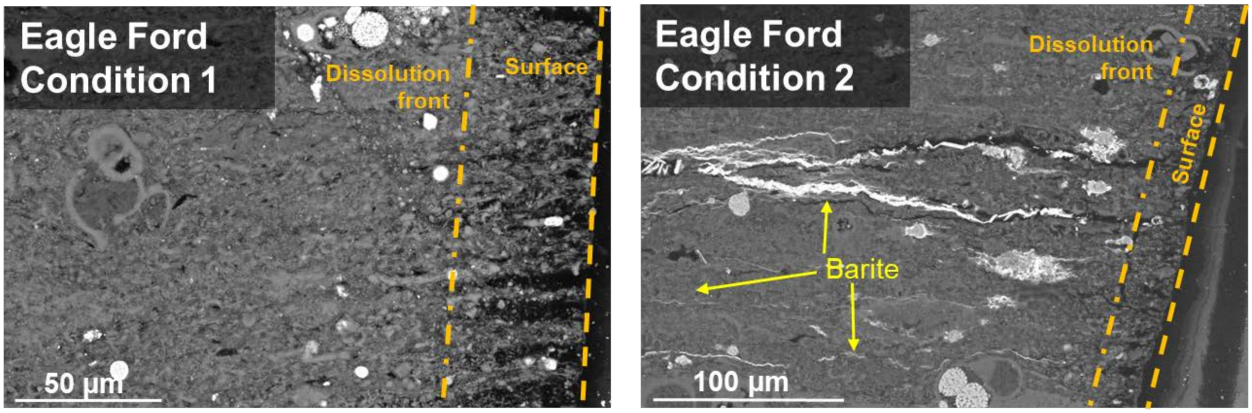

Figure 11. BSE images of post-reaction Eagle Ford cross sections. Condition 1 had no additional barium and sulfate ions in the fracture fluid, and Condition 2 had barium and sulfate ions added into the fracture fluid to promote spontaneous barite precipitation. The images show that under both conditions, the dissolution zones are about 30 μm into the matrix, with obvious secondary porosity from $CaCO_3$ dissolution. Under Condition 2, barite was observed as expected, filling microcracks down to sub-micrometer features.

porosity in the Marcellus cores, SEM-BSE images were taken from the cross section of post-reaction Marcellus (**Figure 10, bottom**). The images show that the observable secondary porosity is localized at large calcite grains (~20 μm diameter) dissolved during the reaction, whereas small secondary pores within the ~100 μm zone are difficult to observe at the SEM-BSE resolution. The $CaCO_3$ dissolution regions in the Eagle Ford are quantified with BSE imaging shown in **Figure 11.** The dissolution rim was about 30 μm wide under both conditions, and has observable increased porosity. Under Condition 2 (i.e., the barite precipitation condition), barite was observed as expected. While barite precipitates filled microcracks in the matrix, they did not fill the secondary porosity from calcite dissolution, suggesting that calcite dissolution was slower than barite precipitation.

In-situ imaging of reaction fronts. For *in-situ* imaging of the reaction front, Eagle Ford microcores were reacted at SSRL beamline 2-2 under dry conditions and reacted for 24 hours with synthetic fracture fluid. Unlike the Marcellus sample where porosity evolution was non-uniform, for the Eagle Ford sample a distinctive reaction front was imaged from the microcore surface inwards (**Figure 12**). These images along with overall changes in whole rock permeability (Task 3&4(b)) indicate that microcracks for high-carbonate/low-clay samples are much less important when reacted with acidic fracture fluids than low-carbonate/high-clay samples such as Marcellus and Eagle Ford.

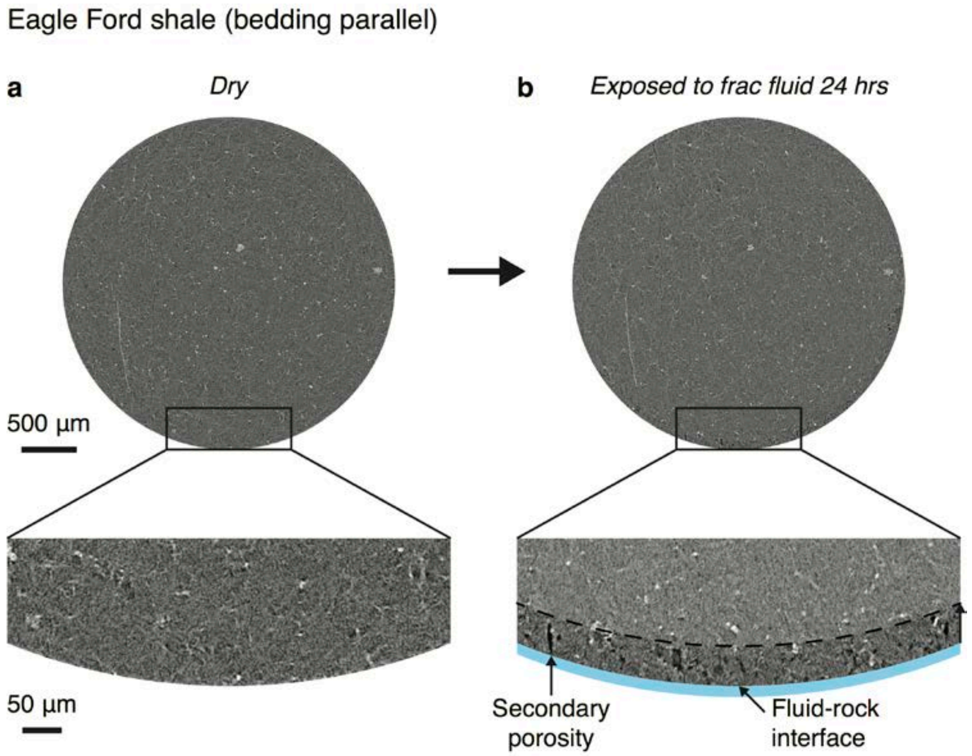

Figure 12: Horizontal cross sections of microtomography images through an Eagle Ford shale core. Bedding is approximately vertical and in and out of the page. (a) Unreacted, dry (b) After 24 hrs exposed to frac fluid. Micron-scale secondary porosity forms in a ~50 µm altered zone along the fluid-rock interface.

In addition to experimental findings, we also completed a URTeC paper. The paper was successfully accepted for publication, and an oral presentation was prepared for URTeC 2018 in July.

Table 3: Objectives in Tasks 3&4 (a) for Quarter 8.

Goal	Status
Initial Draft of Manuscript	Complete

Progress in Quarter 8:

In July, A. Jew presented Q. Li's URTeC slides (URTeC, 2018). The URTeC paper and presentation allowed communication with industry to emphasize the key roles of pH in controlling scaling and oxidation and the necessity of successfully inhibiting secondary minerals that clogs microcracks in the shale matrix.

An initial draft of a journal manuscript under Tasks 3&4(a) is complete. The manuscript presents reactions zone depths with respect to different types of shales and different chemical reactions. This manuscript will be revised to submission to Energy & Fuel to maximize its impact in both academia and industry. In the manuscript, we emphasized that the altered zone is thicker than we previously expected for low-permeable shale samples, and we point out the importance of controlling mineral scaling both at the shale-fluid interface and at least a centimeter deep from the interface into the matrix. Such information is expected to help to increased production efficiency with reduced matrix clogging.

Results in Quarter 8:

Nothing to report

Impact of findings from the past year

Overall, our findings from the past year (Quarter 5-8) under Task 3&4(a) further confirm that although calcite dissolution may substantially open pore spaces and facilitate transport through shale matrices, these opened spaces can be filled with barite and Fe(III) (hydr)oxide minerals that counteract the enhanced transport. In some cases resembling our Eagle Ford system, the microcracks can be severely clogged, reducing transport across shale-fluid interfaces. The pore-filling observations highlights the importance of controlling mineral scaling in the unconventional site to enhance production. Quantitatively, we suggest that investigation on scaling inhibition should focus on not only the shale-fluid interface, but also an altered zone at least 0.5 cm into the matrix, a length scale with observed for both barite perception and sulfide oxidation. Such investigation on scaling inhibition will help industry to maintain permeability of the altered zone in the shale matrix for effective hydrocarbon recovery.

In addition to scaling control, results from the past year on sulfide oxidation confirmed that imbibition of hydraulic fracturing fluids by shale matrix is efficient, and dissolved oxygen in the fracture fluid can participate in important reactions such as pyrite dissolution. Imbibition is critical for estimating relative permeability of hydrocarbon in multiphases hydrocarbon flow, and oxygen-participated reactions may alter pore structure and wettability, both factors indispensable for estimating hydrocarbon recovery efficiency. In summary, with information provided by our study under Task 3&4(a), we expect that investigation on scaling control will be more efficient, and hydrocarbon production will be more accurately predicted.

Plans for the next quarter:

No additional experimentation required. The manuscript draft will be revised and submitted to Energy & Fuels.

Task 3&4 (b): Measuring permeability alteration induced by fracture fluid reaction

For oil/gas production, alteration of the fracture surface microstructure modifies matrix permeability and thus production. In this section, we look at how large is the shale altered zone that is in contact with the reaction fluid and where is it predominantly occurring. We acquired µ-CT imaging of the post-reaction samples to show the altered zone and localization to determine where most of the reaction front is focused. Once the imaging was complete, we performed an assortment of fluid penetration measurements to quantify the porosity changes occurring to the sample. These experiments give us insights showing direct relation of fracture fluid reaction impact on permeability and the SEM/EDS results we have shown in previous reports.

Table 4: Objectives in Tasks 3&4 (b) for Quarter 8.

Goal	Status
No Goals (task complete)	Not Applicable

Progress in Quarters 5-7:

Total rock permeability on shale cores was measured before and after reaction with synthetic fracturing fluid (NETL's Greene Co. recipe) for two shales with highly varied mineralogy. A Marcellus shale sample from PA with < 2 wt.% carbonate and an Eagle Ford shale with > 50 wt.% carbonate was reacted for 6 days at $80^{o}C$ and 77 bar with added $BaCl_2$ and Na_2SO_4 to promote mild barite precipitation. For the low-carbonate/high-clay Marcellus sample, there was a measurable decrease in overall rock permeability due to the closing of interconnected pores, ~19% loss in permeability under reservoir conditions of 2000 PSI pore pressure and 1000 psi effective stress (**Figure 13**). Conversely, the high-carbonate/low-clay Eagle Ford core showed a significant increase in whole rock permeability through the dissolution of carbonate caused by the acidic fracture fluid, ~1-order of magnitude increase in permeability (**Figure 14**).

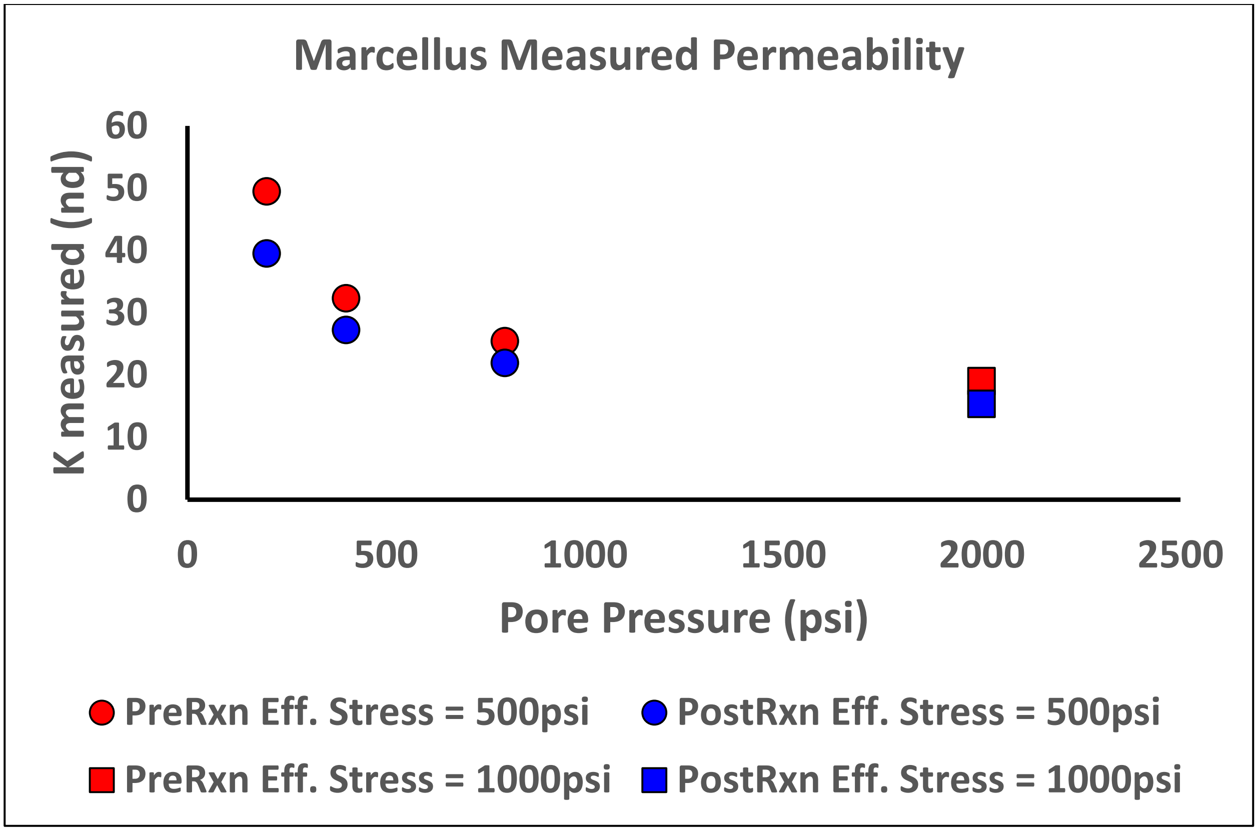

Figure 13: Measured Permeability for pre- and post-reaction Marcellus sample. Reaction conditions were set at 77bar and 80°C for 6 days, with added $BaCl_2$ and Na_2SO_4 salts in place of barite-rich drilling mud to promote barite precipitation. Pulse permeability measurements were acquired at incrementally increasing pore pressures (200psi, 400psi, 800psi) while maintaining an effective pressure=500psi in order to calculate the intrinsic permeability from Klinkenberg analysis. An additional permeability measurement was collected at pore pressure=2000psi and effective pressure=1000psi to replicate relative reservoir production conditions (points with square markers).

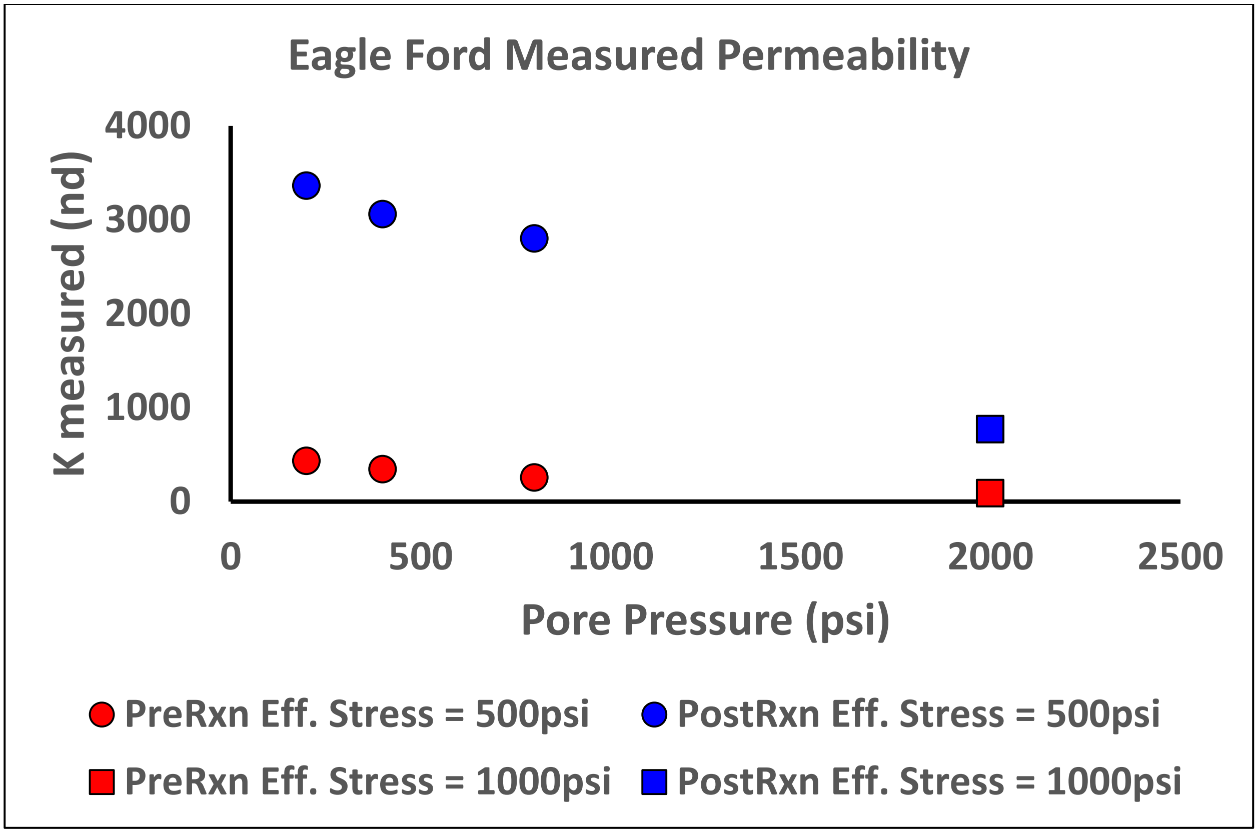

Figure 14: Measured Permeability for pre- and post-reaction Eagle Ford sample. Reaction conditions were set at 77bar and 80°C for 6 days, with added $BaCl_2$ and Na_2SO_4 salts in place of barite-rich drilling mud to promote barite precipitation. Pulse permeability measurements were acquired at incrementally increasing pore pressures (200psi, 400psi, 800psi) while maintaining an effective pressure=500psi in order to calculate the intrinsic permeability from Klinkenberg analysis. An additional permeability measurement was collected at pore pressure=2000psi and effective pressure=1000psi to replicate relative reservoir production conditions. (points with square markers).

To image mineralogical changes on the surface of core samples, SEM with EDS analysis was done on pre- and post-reaction. Energy dispersive analysis of the reacted Marcellus shale surface show significant infilling of pore space and microfractures with barite which is consistent with the reduction in whole rock permeability. The SEM/EDS analysis of the Eagle Ford sample shows significant calcite dissolution along with increased barite precipitation, when compared to Marcellus, occurring throughout the sample (**Figure 15**). These results are consistent with previous work in which it has been shown that higher solution pH promotes more and faster barite precipitation. As reported in our Quarter 7 report (July 2018), fluid penetration measurements show that the overall rock permeability increased because the amount of carbonate dissolved was much greater than the amount of barite precipitating (**Figure 16**). Similar to our findings reported in Tasks 3&4(a) (Calcite Dissolution), these data indicate that barite precipitation is largely complete before calcite dissolution creates large secondary pores.

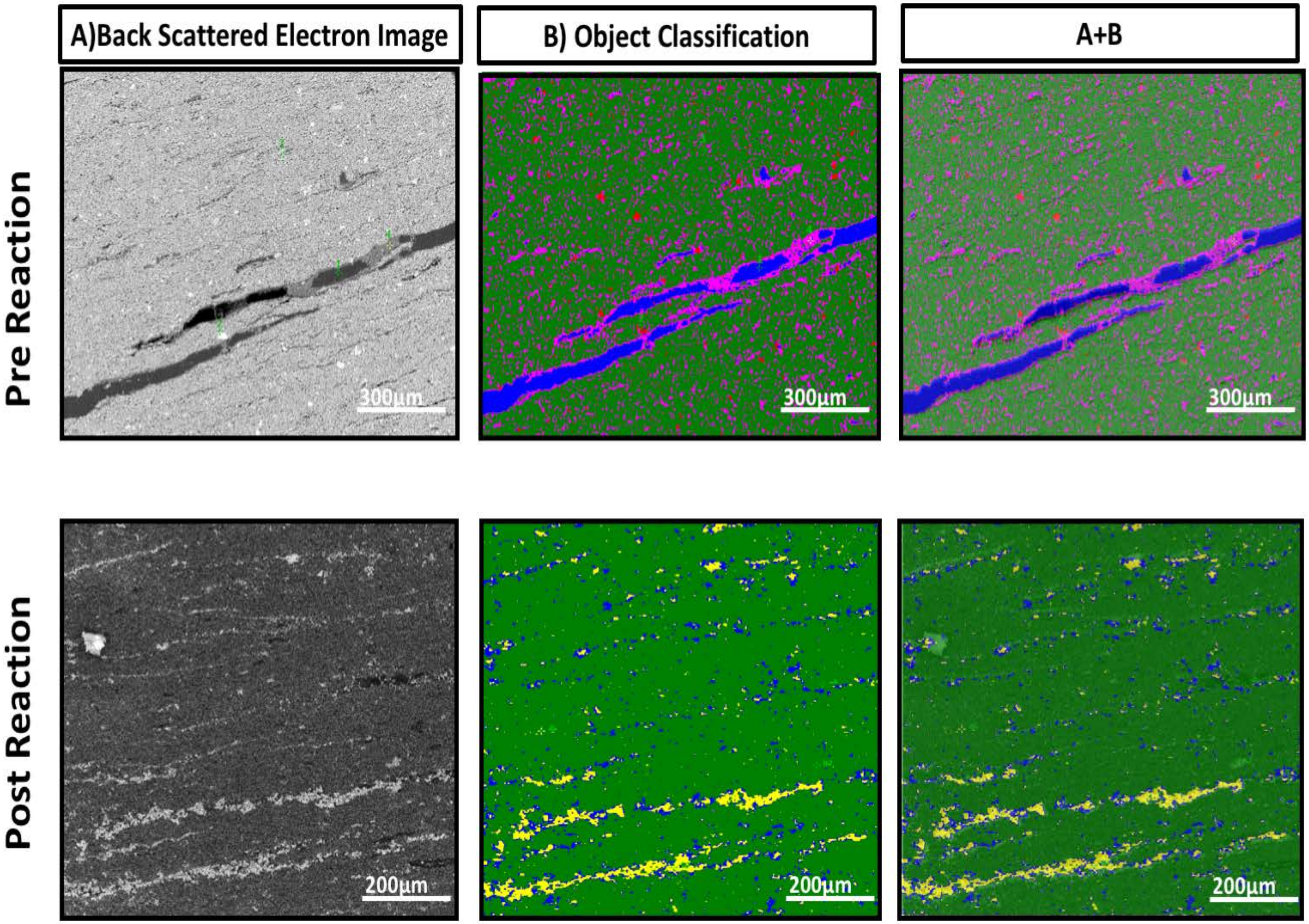

Figure 15: SEM and EDS images for Marcellus pre- (top row) and post-reaction (bottom row) to fracture fluid. Backscattered electron (CBS-a) images emphasize the shale texture and microcracks across the sample (left). The middle column shows object classification derived from EDS cluster analysis. From the overlay of both images (right), we note the barite precipitates deposited into the microcracks as a result of the fracture fluid reaction. Red-Pyrite, Cyan-Carbonate, Purple-Organics, Green-Matrix (Clay, quartz, feldspar, etc.) Yellow-Barite, Blue-Void Space.

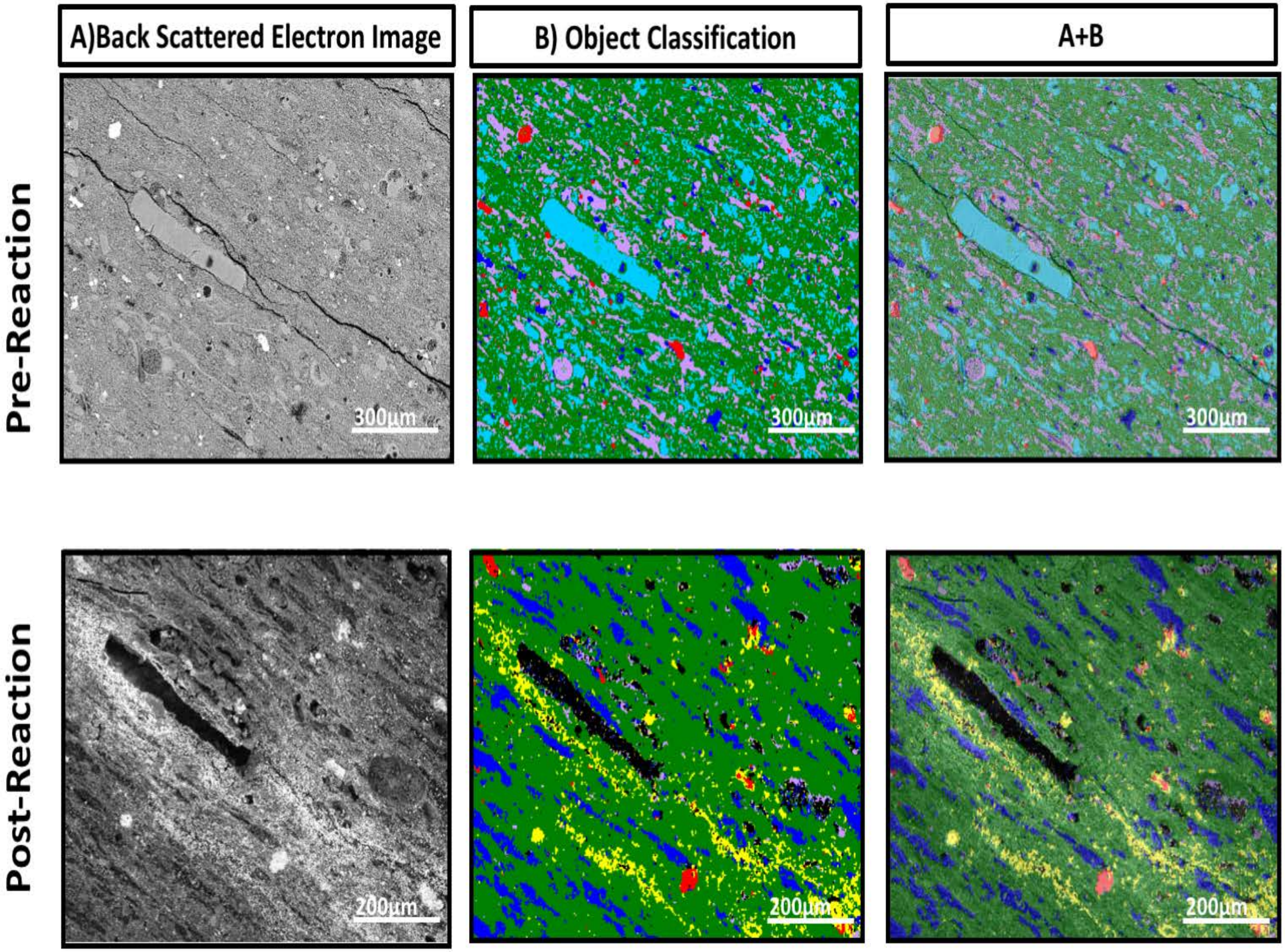

Figure 16: SEM and EDS images for Eagle Ford pre- (top row) and post-reaction (bottom row) to fracture fluid. Backscattered electron (CBS-a) images emphasize the shale texture and microcracks across the sample (left). The middle column shows object classification derived from EDS cluster analysis. From the overlay of both images (right), we note the barite precipitates deposited into the microcracks, with secondary porosity generation (black regions) due to the dissolution of carbonates (cyan) from the fracture fluid reaction Red-Pyrite, Cyan-Carbonate, Purple-Organics, Green-Matrix (Clay, quartz, feldspar, etc.) Yellow-Barite, Blue-Void Space.

As previously shown in Task 3&4(a), microcracks are important for fluid flow in low-carbonate/high-clay samples such as Marcellus and Barnett. X-ray CT images of the Marcellus microcore (reacted) were conducted on the PA sample which is known to contain microcracks. Reconstructed 3D images show the penetration depth of the fracture fluid into the shale core as evidenced by the formation of barite (yellow) (**Figure 17**). Though the majority of the barite precipitation occurred on the surface of the microcore, there was significant penetration into the core through microcracks where barite eventually precipitated, resulting in an overall loss of whole rock permeability.

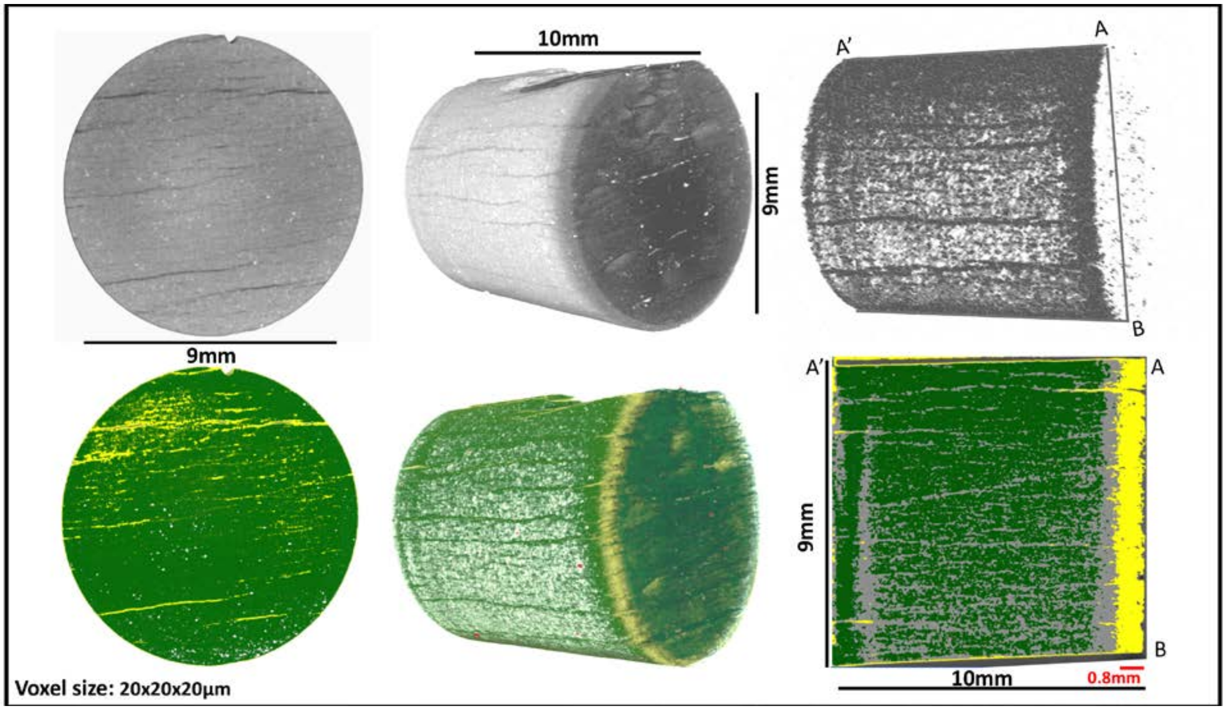

Figure 17: Reconstructed 3D volume from x-ray CT imaging for Marcellus microcore measured with voxel size: 20x20x20µm in greyscale intensity (top row) and color segmented volumes (bottom row). The segmented volumes are colored coded into two main regions: shale matrix and microcracks (green) and reacted zone (yellow). A 2D cross sectional planar view highlighting the depth of penetration of the fracture fluid and barite precipitates into the microcracks is measured around 800µm.

Progress in Quarter 8:

The Ph.D. student working on this section successfully defended his thesis and has begun new employment at Saudi ARAMCO. Prior to his departure he submitted results for this task as a conference manuscript for URTeC 2018.

Results in Quarter 8:

Nothing to report

Impact:

Alteration to the shale due to fracture fluid has a significant impact on whole rock permeability. Both shales illustrate that observed micro-structural changes can be linked to volume averaged properties. Even though significant mineral scale formation (barite) has been seen in the carbonate-rich Eagle Ford samples, the overall shale permeability increased by an order of magnitude due to excessive calcite dissolution. Conversely, in carbonate-poor samples (Marcellus) overall permeability decreased due to mineral scale formation. These results show that mineral scale precipitation in carbonate-rich samples may be of little concern in the short-term (< 1 week) compared to increased mineral dissolution while in clay-rich/carbonate-poor systems mineral scaling must be tightly controlled. Additionally, we have found that microcracks are key to fluid accessing more of the shale matrix. If operators can control fractures (optimizing them for both density and type, focusing on tensile fracturing) more of the shale matrix will be available for production.

Planned Experiments in the next quarter:

No further experiments are planned

Manuscript Plans for Tasks 3&4(b).

URTeC 2018 extended abstract "Effects of Hydraulic Fracturing Fluid Chemistry on Shale Matrix Permeability" has been published and presented.

Task 3&4 (c): Reactive transport modeling of shale-fluid interactions

Chemical modeling of the experimental results is critical for understanding the mechanisms of the system. The modeling process can also extract the important rate laws that can be used for estimating shale-fluid interaction under various condition. In this sub task, we aim at extracting important rate laws for barite precipitation and Fe oxidation, and using these rate laws to simulate shale-fluid interactions in both the sands experiments and whole core experiments.

Progress in Quarters 5-7

Batch models were developed for barite precipitation and Fe oxidation. Data needed for barite precipitation are from Task 2, and data for modeling of Fe oxidation and shale sand reactions were reported in Annual reports in 2016 and 2017 and published in Jew *et al,* (2017) [6] and in Harrison *et al.* (2017) [8].

From the numerical modeling of barite precipitation, we obtained the rate law for barite precipitation and captured the experimental observation that barite precipitation is enhanced with near neutral pH compared to acidic pH. The modeling results match well with the experimental results as shown in **Figure 18**.

The iron oxidation modeling results also match the experimental results with new oxidation rate laws: the first oxidation pathway is pH dependent, where the rate is faster at higher pH, and the second oxidation pathway is bitumen dependent, where the oxidation reaction is catalyzed by the presence of bitumen. The bitumen-dependent rate law is indispensable to simulate Fe(II) oxidation in shale matrix before the acid is completely neutralized, such as in the Marcellus systems. The rate low we obtained from matching modeling results with the experimental data indicate that only a small amount of bitumen is required in order to cause a qualitative change in Fe oxidation behavior. Since virtually all producing shales are relatively enriched in organics, *it* *is likely that organic-promoted oxidation pathways will always control Fe(II) oxidation and scale formation in unconventional reservoirs.*

With these rate laws for Fe oxidation, the model predicts that even at pH 2, a condition that typically does not have Fe oxidation, the existence of bitumen can result in efficient oxidation of 20% of initial Fe(II) to Fe(III) after 48 hours, as observed in the experiments. This model prediction is shown in **Figure 19**.

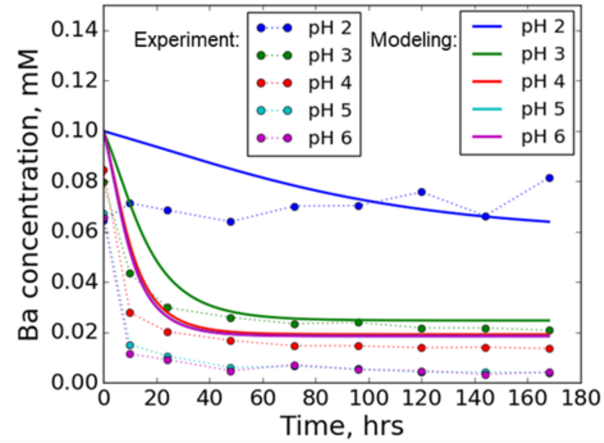

Figure 18. Modeling results for barite precipitation. They match well with the experimental results from Task 2.

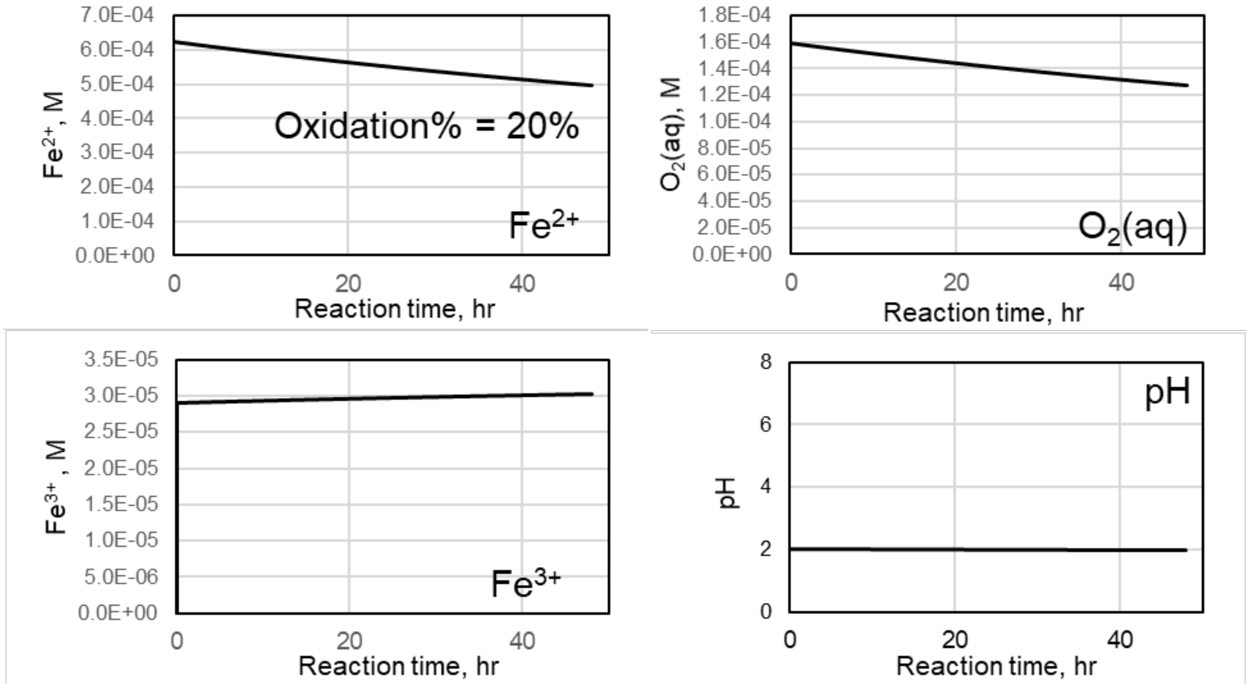

Figure 19. Chemical modeling of Fe oxidation with new rate law. The results show that even at pH 2 when Fe oxidation is typically inhibited, bitumen catalyzed 20% of Fe(II) to Fe(III). This is consistent with the experimental observation.

The rate laws for barite precipitation and Fe oxidation was incorporated into the model for shale sands experiment to capture the time-resolved aqueous chemistry measured in the shale sands experiments. **Figure 20** shows the match of modeling results and experimental results for New York Marcellus and Eagle Ford shale sands interacting with fracture.

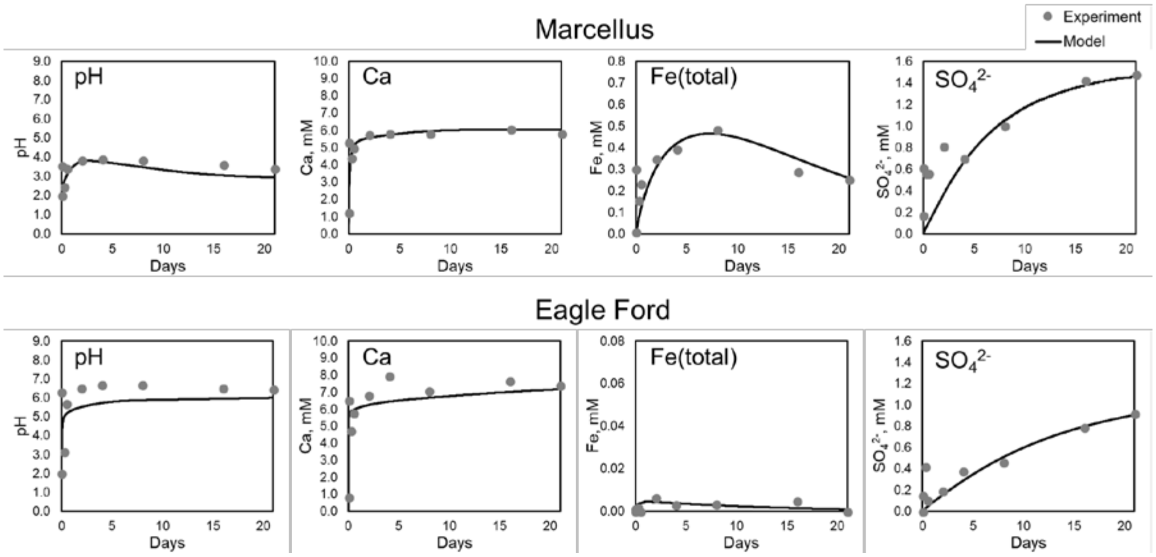

Figure 20. Modeling results compared to experimental data for New York Marcellus (top row) and Eagle Ford (bottom row) sands reacted in fracture fluid for three weeks.

Results in Quarter 8:

Nothing to report.

Impact

Modeling of the experimental observations in the past year (Quarters 5-8) revealed important mechanisms during shale-fluid interactions. For example, it suggests the role of oxygen in controlling pyrite dissolution (thus in sulfide oxidation, Fe oxidation and precipitation, and pH variation due to pyrite dissolution), and further highlighted pH as master parameter in mineral reactions. Understanding these mechanisms guides improvement in unconventional operations, because strategies for enhancing hydrocarbon flow can be designed accordingly with modification of variables (such as pH and oxygen availability) as needed.

In addition to revealing mechanisms, we also obtained the most important kinetic and thermodynamic modeling parameters for barite and Fe(III) (hydr)oxide scaling. Without these parameters, scaling phenomena observed in experiments will not be predicted, and could be completely wrong (i.e., predict no Fe scaling at all for low carbonate Marcellus, contradictory to observation) when applied to unconventional sites. Now these parameters can be applied to shale alteration prediction with enhanced accuracy.

Plans in the next quarter:

- Develop reactive transport models for shale matrix reactions using reaction networks developed in previous quarters.

8. MISCELLANEOUS

Nothing to report.

9. REFERENCES.

[1] Krauss, C., Boom in American Liquefied Natural Gas is Shaking Up the Energy World. *The New York Times*. **2017**, p 6.

[2] Egan, M., America is now the world's largest oil producer. *CNN Business*, September 12, 2018. https://money.cnn.com/2018/09/12/investing/us-oil-production-russia-saudi-arabia/index.html

[3] Technically Recoverable Shale Oil and Shale Gas Resources: An Assessment of 137 Shale Formations in 41 Countries Outside the United States. Report of the U.S. Energy Information Administration, 2013. Washington, DC. 76 pages.

[4] Kondash, A.J.; Lauer, N.E.; Vengosh, A. The intensification of the water footprint of hydraulic fracturing. *Sci. Adv.* **2018**, 4.

[5] Allen, D. T. Atmospheric emissions and air quality impacts from natural gas production and use. *Annu. Rev. Chem. Biomol. Eng.* **2014**, 5 (1) 55– 75.

[6] Jew, A. D.; Dustin, M. K.; Harrison, A. L.; Joe-Wong, C.; Thomas, D. L.; Maher, K.; Gordon E. Brown, J.; Bargar, J. R., *Importance of pH, Oxygen, and Bitumen on the Oxidation and Precipitation of Iron during Hydraulic Fracturing of Oil/Gas Shales*. Energy & Fuels 31(4), **2017**, 3643–3658. **DOI:** 10.1021/acs.energyfuels.6b03220

[7] Vankeuren, A.N.; Hakala, J.A.; Jarvis, K.; Moore, J.E.; Mineral Reactions in Shale Gas Reservoirs: Barite Scale Formation from Reusing Produced Water As Hydraulic Fracturing Fluid. *Environmental Science and Technology* **2017**, 15(16), 9391-9402.

[8] Harrison, A.L.; Jew, A.D.; Dustin, M.K.; Thomas, D.L.; Joe-Wong, C.M.; Bargar, J.R.; Johnson, N.; Brown, G.E.; Maher, K. Element release and reaction-induced porosity alteration during shale-hydraulic fracturing fluid interactions. *Applied Geochemistry* **2017**, 82, 47-62.

[9] Jew, A.D.; Li, Q.; Cercone, D.; Maher, K.; Brown, G.E. Jr.; Bargar, J.R. Barium Sources in Hydraulic Fracturing Systems and Chemical Controls on its Release into Solution. *Unconventional Resources Technology Conference*, **2018**, URTeC: 2899671

[10] Ghode, Roopali; Muley, Rajashree; Sarin, Rajkamal. *Operationally determined chemical speciation of barium and chromium in drilling fluid wastes by sequential extraction*. Chemical Speciation & Bioavailability, 7 (4) **1995**, 133-137.

[11] Neff, Jerry M. *US EPA Report: Fate and biological effects of oil well drilling fluids in the marine environment: A literature review*. **1981**, 1-178.

[12] Neff, Jerry M. *Estimation of bioavailability of metals from drilling mud barite*. Integrated Environmental Assessment and Management. 4 (2) **2008**, 184-193.

[13] Renock, Devon; Landis, Joshua D.; Sharma, Mukul. *Reductive weathering of black shale and release of barium during hydraulic fracturing*. Applied Geochemistry, 65, **2016**, 73-86.

[14] Bai, B.; Carlson, K.; Prior, A.; Douglas, C., Sources of Variability in Flowback and Produced Water Volumes from Shale Oil and Gas Wells. *Journal of Unconventional Oil and Gas Resources*, **2015**, 12, 1-5.

[15] Phan, T.T.; Vankeuren, A.N.; Hakala, J.A., Role of water-rock interaction in the geochemical evolution of Marcellus Shale produced waters. *International Journal of Coal Geology*, **2018**, 191, 95-111.

[16] Zolfaghari, A.; Dehghanpour, J.; Noel, M.; Bearinger, D., Laboratory and Field Analysis of Flowback Water from Gas Shales. *Journal of Unconventional Oil and Gas Resources*, **2016**, 14, 113-127.

[17] Jew, A.D.; Li, Q.; Cercone, D.; Maher, K.; Brown, G.E. Jr.; Bargar, J.R. Barium Sources in Hydraulic Fracturing Systems and Chemical Controls on its Release into Solution. *Unconventional Resources Technology Conference*, **2018**, URTeC: 2899671

[18] Ground Water Protection Council; Interstate Oil & Gas Compact Commission. FracFocus Chemical Disclosure Registry.

[19] Gustafsson, J.P. *Visual MINTEQ*, 2.61; **2009**.

10. RISK ANALYSIS

Task 1: No significant risks to report at this stage of the project.

Task 2: No significant risks to report at this stage of the project.

Task 3&4. No significant risks to report at this stage of the project.

11. MILESTONE STATUS

Activity and milestones	Verification method†	Planned Milestone Date	Actual completion or status
Task 1. Project management			
1.1 Development of PMP	D	10-31-16	10-28-16
1.2 Recruit postdoc / RA	D	4-30-17	10-30-17
1.3 Quarterly research performance reports	D	1-30-17‡	7-30-17
1.4 Annual research performance report	D	11-30-17*	11-30-17
1.5 Final technical report (this report)	D	11-30-18	11-30-18
Task 2. Influence of dissolved organic compounds on precipitate formation/stability			
2.1 Research/evaluation of literature and detailed experimental design	D	1-30-17	12-23-16
2.2 Set-up and test stirred tank reactors	D	1-30-17	12-19-16
2.3 Complete initial scoping experiments to determine types of organic compounds for detailed measurement	D	4-30-17	3-13-17
2.4 Complete measurements of initial rates of solid precipitation	D	7-30-17	6-30-17
2.5 Identification of precipitate mineralogy	XRD, XAS, SEM	10-30-17	9-30-17
2.6 Complete measurement of shale sand dissolution	D	7-30-17	6-30-17
2.7 Complete solubility measurements	D	7-30-17	10-30-17
2.8 Dissolution rate measurements in presence of shale sands with coupled dissolution and precipitation	D	10-30-17	10-30-17
2.9 Complete initial draft of manuscript	D	4-30-18	4-30-18
2.10 Submit manuscript	D	7-30-18	7-30-18
Task 3. Impact of secondary pore networks on gas transport across shale matrix-fracture interfaces			
3.1 Research/evaluation of literature and design experiments favorable for secondary porosity generation	D	1-30-17	12-21-16
3.2 Submit beam time proposals	D	1-30-17	12-1-16
3.3 Acquire shale samples	D	1-30-17	11-9-16
3.4 Conduct telecons quarterly (as needed) with NETL group	N	1-30-17‡	Ongoing
3.5 Conduct telecons quarterly (as needed) with LANL group	N	1-30-17‡	Ongoing
3.6 Mineralogical characterization of shale samples	XRD, SEM	7-30-17	6-30-17
3.7 Measure gas permeability of unreacted cores	P	7-30-17	7-30-17
3.8 Collect μ-CT images for unreacted shale cores	μ-CT	7-30-17	3-7-17
3.9 Complete image processing for unreacted shale cores	D	10-30-17	10-30-17
3.10 Set up and test whole-core reactors: initial scoping experiments	D	7-30-17	11-30-16
3.11 Perform shale whole-core reactions	D	1-30-18	12-19-16
3.12 Collect μ-CT images on reacted cores	μ-CT	4-30-18	12-30-17
3.13 Collect XRM maps on thin section of unreacted and reaction cores	XRM, SEM	4-30-18	4-30-18
3.14 Measure gas permeability through reacted cores	P	4-30-18	4-30-18
3.15 Complete image processing and data analysis for reacted cores	D	9-30-18	9-30-18
3.16 Develop a shale sand batch reaction model to refine rate constants for new Fe(II) oxidation rate law	D	7-30-18	7-30-18
3.17 Complete initial draft of manuscript	D	9-30-18	9-30-18
3.18 Submit manuscript	D	12-30-18	

Activity and milestones	Verification method[†]	Planned Milestone Date	Actual completion or status
Task 4. Impact of secondary precipitation on gas transport across shale matrix-fracture interfaces			
4.1 Research/evaluation of literature and design experiments favorable for secondary precipitation	D	1-30-17	12-21-16
4.2 Measure gas permeability of unreacted cores	P	7-30-17	7-30-17
4.3 Collect μ-CT images on unreacted shale cores	μ-CT	7-30-17	3-7-17
4.4 Complete image processing and analysis on unreacted shale cores	D	10-30-17	10-30-17
4.5 Set up and test whole-core reactors: initial scoping experiments	D	10-30-17	3-20-17
4.6 Perform shale whole-core reactions	D	4-30-18	4-30-18
4.7 Measure permeability of reacted cores	D	9-30-18	3-30-18
4.8 Collect μ-CT images on reacted cores	P, μ-CT	10-30-18	3-30-18
4.9 Collect XRM maps on thin section of unreacted and reaction cores	XRM, SEM	10-30-18	7-30-18
4.10 Complete image processing and data analysis for reacted cores	D	3-31-19	9-30-18
4.11 Develop a batch reaction model to refine rate constants for barite scale precipitation reactions	NM	10-30-18	3-30-18
4.12 Build a 1D reactive transport model for shale matrix-fluid interface reactions	D	12-30-18	In progress

[‡] Quarterly reports will follow every 3 months following starting date. * Annual reports are due every 12 months on Nov 30.

[†] Verification Method Key:

AF = Software for data processing and visualization (Avizo Fire)
D = Documentation or data
EELS = Electron energy loss spectroscopy
FIB-SEM = Focused ion beam – scanning electron microscopy
μ-CT = Micrometer-scale X-ray computed tomography
nano-CT = Nanometer-scale X-ray computed tomography
N = Note from meeting
NM = Numerical modeling
OP = Optical petrography
P = Pulse-decay permeability
SAXS = Small angle X-ray scattering
SANS = Small angle neutron scattering
SEM = Scanning electron microscopy
TEM = Transmission electron microscopy
TXMWiz = Software for data processing of transmission X-ray images (TXM Wizard)
XAS = X-ray absorption spectroscopy
XRM = X-ray microprobe
XRD = X-ray diffraction

12. SCHEDULE STATUS

All milestones for this quarter have been met. As of the time of writing, the project is on-schedule.

Changes to schedule and milestones in the past quarter: Qingyun Li (postdoc) took a 2-month maternity leave from mid-June to mid-August. The affected subtasks were rescheduled accordingly, as approved in May 2018 and noted in the report for Quarter 6 (May 15, 2018).

Cumulative modification explanation log for milestones list:

Report Date	Task	Planned date	Revised date	New Task goal / Explanation
5-15-18	3.15	7-30-18	9-30-18	Accommodate 2-month maternity leave
5-15-18	3.16	7-30-18	9-30-18	Accommodate 2-month maternity leave New task name: “Develop a shale sand batch reaction model to refine rate constants for new Fe(II) oxidation rate law”
5-15-18	3.17	7-30-18	9-30-18	Accommodate 2-month maternity leave
5-15-18	3.18	10-31-18	12-31-18	Accommodate 2-month maternity leave
5-15-18	4.10	1-31-19	3-31-19	Accommodate 2-month maternity leave
5-15-18	4.11	10-31-18	NA	New task name: Develop a batch reaction model to refine rate constants for barite scale precipitation reactions
5-15-18	4.12	NA	12-31-18	New task: Build a 1D reactive model for shale matrix-fluid interface reactions

Project timeline from the Project Management Plan. “M” denotes milestones.

Task	Title	Month of project																													
		2016			2017													2018												2019		
		1	2	3	4	5	6	7	8	9	10	11	12	13	14	15	16	17	18	19	20	21	22	23	24	25	26	27	28	29	30
		Oct	Nov	Dec	Jan	Feb	Mar	Apr	May	Jun	Jul	Aug	Sep	Oct	Nov	Dec	Jan	Feb	Mar	Apr	May	Jun	Jul	Aug	Sep	Oct	Nov	Dec	Jan	Feb	Mar
1	**Project management plan**																														
1.1	Development of PMP	🟥	🟥	🟥	🟥	🟥	🟥	🟥	🟥	🟥	🟥	🟥	🟥	🟥	🟥	🟥	🟥	🟥	🟥	🟥	🟥	🟥	🟥	🟥	🟥						
1.2	Recruit postdoc/RA	🟥	🟥	🟥	🟥	🟥	🟥	🟥																							
1.3	Quarterly research performance reports				🟥			🟥			🟥						🟥			🟥			🟥								
1.4	Annual research performance report														🟥												🟥				
1.5	Final technical report																										🟥				
2	**Influence of dissolved organic compounds on precipitate formation/stability**																														
2.1	Evaluate literature/ experimental design	🟥	🟥	🟥	🟥																										
2.2	Set-up and test stirred tank reactors	🟥	🟥	🟥	🟥																										
2.3	Complete initial scoping experiments				🟥	🟥	🟥	🟥																							
2.4	Complete measurements of initial rates of solid precipitation							🟥	🟥	🟥	🟥																				
2.5	Identification of precipitate mineralogy										🟥	🟥	🟥	🟥																	
2.6	Measure shale sand dissolution							🟥	🟥	🟥	🟥																				
2.7	Complete solubility measurements									🟥	🟥																				
2.8	Dissolution rate measurements in presence of shale sands										🟥	🟥	🟥	🟥																	
2.9	Complete initial draft of manuscript													🟥	🟥	🟥	🟥	🟥	🟥	🟥											
2.10	Submit manuscript																			🟥	🟥	🟥	🟥								
3	**Impact of secondary pore networks on gas transport across shale matrix-fracture interfaces**																														
3.1	Evaluate literature/ experimental design	🟥	🟥	🟥	🟥																										
3.2	Submit beam time proposals	🟥	🟥	🟥	🟥																										
3.3	Acquire shale samples	🟥	🟥	🟥	🟥																										
3.4	Quarterly (as needed) with NETL group				🟥			🟥			🟥						🟥			🟥			🟥								
3.5	Quarterly (as needed) with LANL group				🟥			🟥			🟥						🟥			🟥			🟥								
3.6	Mineral characterization shale samples				🟥	🟥	🟥	🟥	🟥	🟥	🟥																				
3.7	Measure permeability of unreacted cores				🟥	🟥	🟥	🟥	🟥	🟥	🟥																				
3.8	Collect µ-CT images, unreacted cores				🟥	🟥	🟥	🟥	🟥	🟥	🟥																				
3.9	Image processing, unreacted shale cores							🟥	🟥	🟥	🟥	🟥	🟥	🟥																	
3.10	Test whole-core reactors: Initial scoping experiments				🟥	🟥	🟥	🟥	🟥	🟥	🟥																				
3.11	Perform shale whole-core reactions										🟥	🟥	🟥	🟥	🟥	🟥	🟥														
3.12	Collect µ-CT images on reacted cores															🟥	🟥	🟥	🟥	🟥											
3.13	XRM maps, unreacted/ reacted cores				🟥	🟥	🟥	🟥	🟥	🟥	🟥	🟥	🟥	🟥	🟥	🟥	🟥	🟥	🟥	🟥											
3.14	Measure permeability of reacted cores															🟥	🟥	🟥	🟥	🟥											
3.15	Image processing, reacted shale cores																	🟥	🟥	🟥	🟥	🟥	🟥	🟥	🟥						
3.16	Develop a batch reaction model to refine rate constants for Fe(II) oxidation			🟥	🟥	🟥	🟥	🟥	🟥	🟥	🟥	🟥	🟥	🟥	🟥	🟥	🟥	🟥	🟥	🟥	🟥	🟥	🟥	🟥	🟥						
3.17	Complete initial draft of manuscript																	🟥	🟥	🟥	🟥	🟥	🟥	🟥	🟥						
3.18	Submit manuscript																					🟥	🟥	🟥	🟥	🟥	🟥	🟥			
4	**Impact of matrix precipitation on gas transport across shale matrix-fracture interfaces**																														
4.1	Evaluate literature/ experimental design	🟥	🟥	🟥	🟥																										
4.2	Measure permeability of unreacted cores				🟥	🟥	🟥	🟥	🟥	🟥	🟥																				
4.3	Collect µ-CT images, unreacted cores				🟥	🟥	🟥	🟥	🟥	🟥	🟥																				
4.4	Image processing, unreacted shale cores							🟥	🟥	🟥	🟥	🟥	🟥	🟥																	
4.5	Test whole-core reactors: Initial scoping experiments							🟥	🟥	🟥	🟥	🟥	🟥	🟥																	
4.6	Perform shale whole-core reactions												🟥	🟥	🟥	🟥	🟥	🟥	🟥	🟥											
4.7	Measure permeability of reacted cores																		🟥	🟥	🟥	🟥	🟥	🟥	🟥						
4.8	Collect µ-CT images on reacted cores																					🟥	🟥	🟥	🟥	🟥	🟥	🟥			
4.9	XRM maps, unreacted/ reacted cores																					🟥	🟥	🟥	🟥	🟥	🟥	🟥			
4.10	Image processing, reacted shale cores																							🟥	🟥	🟥	🟥	🟥	🟥	🟥	🟥
4.11	Develop a batch reaction model to refine rate constants for barite scale							🟥	🟥	🟥	🟥	🟥	🟥	🟥	🟥	🟥	🟥	🟥	🟥	🟥	🟥	🟥	🟥	🟥	🟥	🟥	🟥	🟥			
4.12	Build a 1D reactive model for shale matrix-fluid interface reactions							🟥	🟥	🟥	🟥	🟥	🟥	🟥	🟥	🟥	🟥	🟥	🟥	🟥	🟥	🟥	🟥	🟥	🟥	🟥	🟥	🟥			

13. COST STATUS

Cost Plan/Status									
Basesline Reporting Quarter		Year 4	Start: 10/1/16	End: 9/30/17		Year 5	Start: 10/1/17	End: 9/30/18	
		Q1	Q2	Q3	Q4	Q5	Q6	Q7	Q8
Baseline Cost Plan									
Federal Share	Task 1	$ 9,686	$ 9,686	$ 9,686	$ 9,686	$ 12,750	$ 12,750	$ 12,750	$ 12,750
	Task 2	$ 31,681	$ 31,681	$ 31,681	$ 31,681	$ 44,625	$ 44,625	$ 44,625	$ 44,625
	Task 3	$ 42,400	$ 42,400	$ 42,400	$ 42,400	$ 35,700	$ 35,700	$ 35,700	$ 35,700
	Task 4	$ 23,733	$ 23,733	$ 23,733	$ 23,733	$ 34,425	$ 34,425	$ 34,425	$ 34,425
	Task 5								
	Task 6								
Non-Federal Share									
Total Planned Costs (Federal and Non-Federal)									
Cumulative Baseline Cost		$ 107,500	$ 215,000	$ 322,500	$ 430,000	$ 557,500	$ 685,000	$ 812,500	$ 940,000
Actual Incurred Costs									
Federal Share	Task 1	$ 7,290	$ 13,437	$ 8,509	$ 16,530	$ 14,370	$ 9,979	$ 12,291	$ 13,261
	Task 2	$ 25,514	$ 47,028	$ 29,782	$ 57,855	$ 50,294	$ 34,927	$ 43,019	$ 46,414
	Task 3	$ 20,411	$ 37,622	$ 23,826	$ 46,284	$ 40,236	$ 27,942	$ 34,415	$ 37,132
	Task 4	$ 19,682	$ 36,279	$ 22,975	$ 44,631	$ 38,799	$ 26,944	$ 33,186	$ 35,805
	Task 5	$ -	$ -	$ -	$ -	$ -	$ -	$ -	$ -
	Task 6	$ -	$ -	$ -	$ -	$ -	$ -	$ -	$ -
Non-Federal Share									
Total Incurred Costs - Quarterly (Federal and Non-Federal)									
Cumulative Incurred Cost		$ 72,898	$ 134,366	$ 85,093	$ 165,300	$ 143,698	$ 99,792	$ 122,912	$ 132,613
Variance									
Federal Share	Task 1	$ 2,396	$ (3,750)	$ 1,177	$ (6,843)	$ (1,620)	$ 2,771	$ 459	$ (511)
	Task 2	$ 6,167	$ (15,347)	$ 1,899	$ (26,174)	$ (5,669)	$ 9,698	$ 1,606	$ (1,789)
	Task 3	$ 21,988	$ 4,777	$ 18,574	$ (3,884)	$ (4,536)	$ 7,758	$ 1,285	$ (1,432)
	Task 4	$ 4,050	$ (12,546)	$ 758	$ (20,898)	$ (4,374)	$ 7,481	$ 1,239	$ (1,380)
	Task 5	$ -	$ -	$ -	$ -	$ -	$ -	$ -	$ -
	Task 6	$ -	$ -	$ -	$ -	$ -	$ -	$ -	$ -
Non-Federal Share		$ -	$ -	$ -	$ -	$ -	$ -	$ -	$ -
Total Variance - Quarterly (Federal and Non-Federal)		$ -	$ -	$ -	$ -	$ -	$ -	$ -	$ -
Cumulative Variance		$ 52,503	$ 25,637	$ 48,044	$ (9,755)	$ (25,953)	$ 1,755	$ 6,343	$ 1,230

14. COLLABORATIVE LEVERAGING.

Collaboration on research activities is an important method to leverage the investment in this project. We are collaborating with 1 Ph.D. student in the Zoback research group at Stanford University. This project is also being leveraged by DOE-FE programs for HFTS-II and the LBNL-LLNL multiscale unconventional modeling project. Importantly, our ongoing ad-hoc collaboration with the Hakala and Lopano group at NETL has been very productive. Our collaboration with Pioneer Natural Resources is providing invaluable insights into injection chemistry, injection sequences, volumes, and rates that are critical in order to understand what operators are doing in highly complex unconventional oil systems. We are also collaborating with a new Stanford University EFRC project led by Dr. Kovscek of the department of energy resources engineering.

15. CONCLUSIONS

Over the past year, we continued to advance robustly towards our project goals. The first of these goals was to discover, quantify, and develop models to describe geochemical controls over barite scale precipitation in fracture-stimulated shales. At the end of FY 2017, we provided evidence that barite-infused drilling mud is likely to be an important source of Ba^{2+} and sulfate to fracture fluids and developed a conceptual model for barium cycling in stimulated unconventional reservoirs. In FY 2018, we used these models to predict that substitution of sulfuric acid for hydrochloric acid should strongly reduce barite leaching from drilling mud. Our subsequent experimental program confirmed this prediction. Moreover, thermodynamic calculations indicate that barite leaching can be effectively mitigated by replacing of only 10% of the hydrochloric acid with sulfuric acid. The incremental nature of this finding is extremely important to coaxing industrial producers to implement because small changes that provide big benefits more easily gain acceptance and are less expensive to implement than large-scale changes.

These findings provided the basis for a provisional patent filed in Quarter 4. These findings also allowed us to improve our conceptual model for barium cycling, which we used to make new predictions to show the impact of adding small amounts of sulfuric acid to the acid spearhead.

Our research to probe the altered zone at shale fracture surfaces has produced several important findings. When microfractures are present, alteration can occur to depths of cm into shale fracture surfaces, suggesting that these features will be very important to strategies designed to manipulate access to matrix. Different reaction fronts penetrate to different depths, with both pyrite oxidation and barite precipitation evident deep within matrix. Barite also was observed as very thin (40 µm thick) fracture surface coatings. When these coatings were present, the permeability of Marcellus shales decreased by 20%. On the other hand, carbonate-rich Eagle Ford shale, permeability increased by about an order of magnitude when carbonate grains were dissolved by acid, even though barite scale was present as surfaces coatings and microfracture infilling. This finding indicates that the extent and/or timing of mineral scale precipitation relative to generation of porosity is important.

Overall, these results provide a firm foundation from which to launch our new Basin-Specific Geochemistry research program. We will expand the mineral scale precipitation studies to account for conditions specific to basins and stimulation practices. We will extend our work on the altered zone to develop strategies to manipulate this region to improve recovery factors.

APPENDIX A. Deliverables

Patents.

1. Provisional Patent (2018)- Fracture Fluid Alteration to Mitigate Barite Scale Precipitation in Unconventional Oil/Gas Shale Systems. Patent ID: 62/717326

Manuscripts published, submitted, or in revision.

URTeC Extended Abstracts (2018)-

2. Barium Sources in Hydraulic Fracturing Systems and Chemical Controls on its Release into Solution. A.D. Jew, Q. Li, D. Cercone, K. Maher, G.E. Brown, Jr., and J.R. Bargar. URTEC-2899671-MS. Extended Abstracts of the 2018 Unconventional Resources Technology Conference 2018, 2899671, DOI doi:10.15530/URTEC-2018-2899671.

3. Imaging Pyrite Oxidation and Barite Precipitation in Gas and Oil Shales. Q. Li, A.D. Jew, A.M. Kiss, A. Kohli, A. Alalli, A.R. Kovscek, M.D. Zoback, D. Cercone, K. Maher, G.E. Brown, Jr., and J.R. Bargar. URTEC-2902747-MS. Extended Abstracts of the 2018 Unconventional Resources Technology Conference 2018, 2902747, DOI https://doi.org/10.15530/URTEC-2018-2902747.

4. Effects of hydraulic fracturing fluid on shale matrix permeability. A. Alalli, Q. Li, A.D. Jew, A. Kholi, J.R. Bargar, and M. Zoback. URTEC-2881314-MS. Extended Abstracts of the 2018 Unconventional Resources Technology Conference 2018, 2881314, DOI https://doi.org/10.15530/URTEC-2018-2881314.

Energy & Fuels (2018)-

5. Shale Kerogen-Hydraulic Fracturing Fluid Interactions and Contaminant Release. Megan K. Dustin, Adam D. Jew, Anna L. Harrison, Claresta Joe-Wong, Dana L. Thomas, Katharine Maher, Gordon E. Brown, Jr., John R. Bargar, *Energy and Fuels*. Vol. **32**, No. 9, 8966-8977. DOI: 10.1021/acs.energyfuels.8b01037.

6. Organic and Inorganic Controls on Barite Precipitation in Hydraulic Fracturing Systems. Adam D. Jew, Qingyun Li, Kate Maher, Gordon E. Brown, Jr., John R. Bargar

Manuscripts in preparation.

Environmental Science & Technology-

7. The Effect of Hydraulic Fracturing Fluid on the Stability of Uranium in Unconventional Oil/Gas Shales. Adam D. Jew, Clemence J. Besancon, Scott J. Roycroft, Vincent S. Noel, Gordon E. Brown, Jr., John R. Bargar

Energy & Fuel-

8. Quantification of alteration depths in shale matrices after injection of hydraulic fracturing fluid. Qingyun Li, Adam D. Jew, Arjun Kohli, Kate Maher, Gordon E. Brown Jr., John R. Bargar.

Presentations at National Meetings.

9. Presented research at the NETL/DOE meeting: Mastering the subsurface through technology innovation partnerships and collaboration: carbon storage and oil and natural gas technologies review meeting. Aug. 13-16, 2018. Pittsburgh, PA

10. AIChE Annual Meeting, Oct. 29-Nov. 3, 2017, Minneapolis, MN. Adam D. Jew, David Cercone, Qingyun Li, Megan K. Dustin, Anna L. Harrison, Claresta Joe-Wong, Dana L. Thomas, Kate Maher, Gordon E. Brown, Jr., John R. Bargar. *Chemical controls on secondary mineral precipitation of Fe and Ba in hydraulic fracturing systems.*

11. AGU Fall Meeting, Dec. 11-15, 2017, New Orleans, LA. Qingyun Li, Adam D. Jew, Gordon E. Brown, Jr., John R. Bargar. *Chemical reactivity of shale matrixes and the effects of barite scale formation*

12. DOE Upstream Workshop, Feb. 14, 2018, Houston, TX. Alexandra Hakala, Joe Morris, John Bargar, Jens Birkholzer. *Fundamental Shale Interactions-DOE National Laboratory Research*

URTeC Conference, July 23-25, 2018, Houston, TX:

13. Adam D. Jew, Qingyun Li, David Cercone, Kate Maher, Gordon E. Brown, Jr., John R. Bargar. *Barium Sources in Hydraulic Fracturing Systems and Chemical Controls on its Release into Solution*.

14. Qingyun Li, Adam D. Jew, Andrew M. Kiss, Arjun Kohli, Abdulgader Alalli, Anthony R. Kovscek, Mark D. Zoback, David Cercone, Katharine Maher, Gordon E. Brown, Jr., John R. Bargar. *Imaging Pyrite Oxidation and Barite Precipitation in Gas and Oil Shales*

15. Abdulgader Alalli, Qingyun Li, Adam Jew, Arjun Kholi, John R. Bargar, Mark Zoback. *Effects of hydraulic fracturing fluid on shale matrix permeability*.

Other activities.

- Participant in DOE-FE Oil and Natural Gas Knowledge Management adviser group (A. Jew)
- Participant in DOE-FE Oil and Natural Gas Science Leadership adviser group (J. Bargar)